FLUX PERTURBATION BY GOLD FOILS

by

Robert Mansfield Mills

A Thesis Submitted to the
Graduate Faculty in Partial Fulfillment of
The Requirements for the Degree of
MASTER OF SCIENCE

Major Subject: Nuclear Engineering

Approved:

Signatures have been redacted for privacy

Iowa State University
Of Science and Technology
Ames, Iowa

1962

TABLE OF CONTENTS

I. INTRODUCTION

The object of this thesis is to determine whether or not the perturbation (depression) of the thermal portion of a neutron flux will be affected by changes in the energy distribution of the flux as measured by the cadmium ratio. Gold foils in a graphite medium were chosen for this experiment.

In the field of nuclear engineering accurate measurements of the magnitude of a neutron flux are often required. One of the standard methods of measuring this flux requires the use of a thin metallic foil called a neutron detector foil. The detector foil is used to measure the neutron flux by means of induced radioactivity. The foil is placed in the neutron flux where it absorbs neutrons, producing a nuclide which is radioactive. The activity of this radioactive product can then be measured. This induced activity is directly related to the magnitude and energy distribution of the neutron flux.

However, in absorbing some of the neutrons from the flux, the detector foil depresses the flux. Therefore, the foil does not measure the actual undisturbed flux, but it measures the depressed or perturbed flux. This disturbance is called flux perturbation.

The ratio of the average flux through the foil to the unperturbed flux in the absence of the foil is the flux perturbation factor. This flux perturbation factor has been found to vary in relation to a number of factors all of which affect the actual measurement of the flux. Some of these factors are foil material, size, thickness, and density; properties of the surrounding medium; and energy and angular distribution of the flux.

To simplify the variable factor of energy distribution of the flux, only thermal fluxes will be considered in this thesis. In the case of a gold detector foil this can be accomplished experimentally in either of two ways; by placing the foil in a thermal flux or by subtracting the resonance activity (obtained by irradiating the foil enclosed in a cadmium cover) from the total activity (obtained by irradiating the bare foil).

The cadmium ratios of the fluxes measured at positions 1 and 2 were 1534 and 125 respectively. Even at a cadmium ratio of 125, only 1/125 of the flux was above thermal or epi-cadmium. Therefore, the flux at these positions was considered almost entirely thermal. Since the flux was thermalized in a diffusion medium, it should have approximately a Maxwellian energy distribution.

The thermal flux obtained by the cadmium difference method should have a slightly different energy distribution than the flux that was almost entirely thermalized by the diffusion medium.

The perturbation factors obtained for gold foils in graphite acted on by a thermal flux have been fairly well established.

The purpose of this thesis is to determine whether or not these perturbation factors determined from thermal fluxes can be applied directly to the thermal or subcadmium portion of a total flux containing neutrons in a wide range of energies.

To measure the perturbation factor stacks of foils of varying thicknesses were placed in the graphite thermal column of the UTR-10 reactor and activated. By extrapolating the value of the flux measured down to zero thickness of detector foil, the unperturbed flux could be determined. Since the flux had been measured with the varying thicknesses of stacks of detector foils, the effect of foil thickness on the perturbation factor could be seen.

To determine the effect of changes in cadmium ratio on the perturbation factor, the stacks of detector foils were placed at four different positions along the center of the thermal column. The cadmium ratio varies along the thermal column from about 4 to 1500. A greater portion of the flux in the thermal column is thermal at positions further from the core of the reactor.

The perturbation of the flux was found to increase greatly as the foil stack thickness was increased. Plots of the flux perturbation factor vs. foil thickness showed that the perturbation for the thermal portion of the flux (that below the Gd cutoff energy) was fairly close to that predicted by theory and to that obtained by other experimenters.

Therefore, it was concluded that the perturbation factors measured for thermal fluxes (cadmium ratio equal to 125 or greater) could be applied to the thermal portion of fluxes measured at low cadmium ratios.

A discrepancy occurred in the results for the perturbation factors obtained in thermal fluxes. The perturbation factors were too great compared to the results of other experimenters and compared to the perturbation factors obtained for the thermal portion of fluxes with low cadmium ratios.

No definite explanation for this discrepancy could be determined.

II. REVIEW OF LITERATURE

The problem of flux perturbation by detector foils has been studied by many authors who obtained widely varying results. In the earlier investigations (1, 7, 9, 10) much of this variation in results was due to a lack of agreement in the definition of the perturbation factor and to different methods of approach to the problem.

However, in the past few years a fair amount of agreement has been attained. When modified, many of the results, even of earlier investigators, are found to agree fairly well with each other and with the theories presented by such investigators as Bothe (1) and Skyrme (7). (See Table 1.)

The more widely accepted theory is that the flux perturbation consists of two effects superimposed on each other. The first of these effects consists of a depression of the flux in the neighborhood of the foil. This local depression is caused by absorption of neutrons by the foil; thus lowering the density of neutrons available near the foil. This effect is sometimes described as shadowing. In an isotropic system neutrons which are absorbed by the detector foil are not later available to diffuse back to the area of the foil. Also a neutron which enters the foil from one side and is absorbed by the foil will not be present to contribute to the neutron flux on the other side of the foil--thus the shadowing effect. This effect is called "flux depression, H".

Table 1. Flux perturbation for circular gold foils[a] in graphite

	Foil thicknesses (in mils)							
	1	2	3	4	5	10	15	20
Sola (measured)	0.951	0.925	0.905	0.883	0.864	0.788	0.733	0.683
Bothe (calculated)	0.968	0.936	0.915	0.893	0.872	0.792	0.731	0.675
Skyrme (calculated)	0.962	0.933	0.907	0.883	0.862	0.763	0.678	0.587

[a]All foils were 1/2 inch in diameter.

(See Figure 1.)

The second of the two effects which contribute to flux perturbation is caused by the attenuation of the neutron flux as it penetrates the foil so that the interior of the foil has a lower saturated activity than the surface layers. This effect is called "self shielding, G".

The total effect then of both "flux depression H" and "self-shielding G" is "flux perturbation, F". F = (G)(H).

Initial investigation of the problem of flux perturbation was conducted by Bothe (1). He simplified the problem by assuming that the flux is originally constant throughout the medium and that first-order diffusion theory can be used to determine the movement of the neutrons in the medium. Bothe developed his equations on the basis of a spherical detector and then related them to a disc. His final result for the self-shielding factor is

$$G = \frac{1-e^{-x}(1-x)-x^2E_1(x)}{2x}$$

where x is the foil thickness measured in mean-free-path units and

$$E_1(x) = \int_x^\infty \frac{e^{-s}}{s}\,ds$$

G is found by considering the foil to be a thin plane infinite in extent in an unperturbed isotropic flux. Since the foils used are not infinite in extent some error is introduced. However, other investigators (7) have found that the

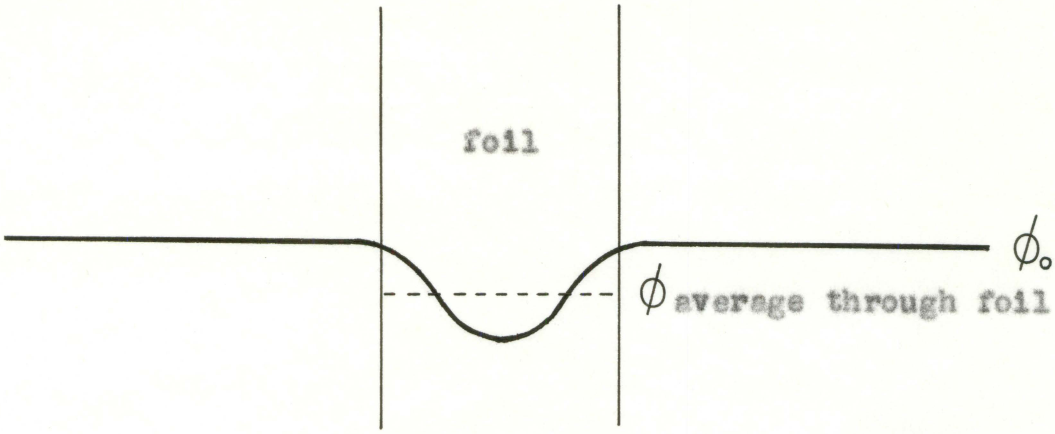

(a) Partial flux-perturbation due to self-shielding only

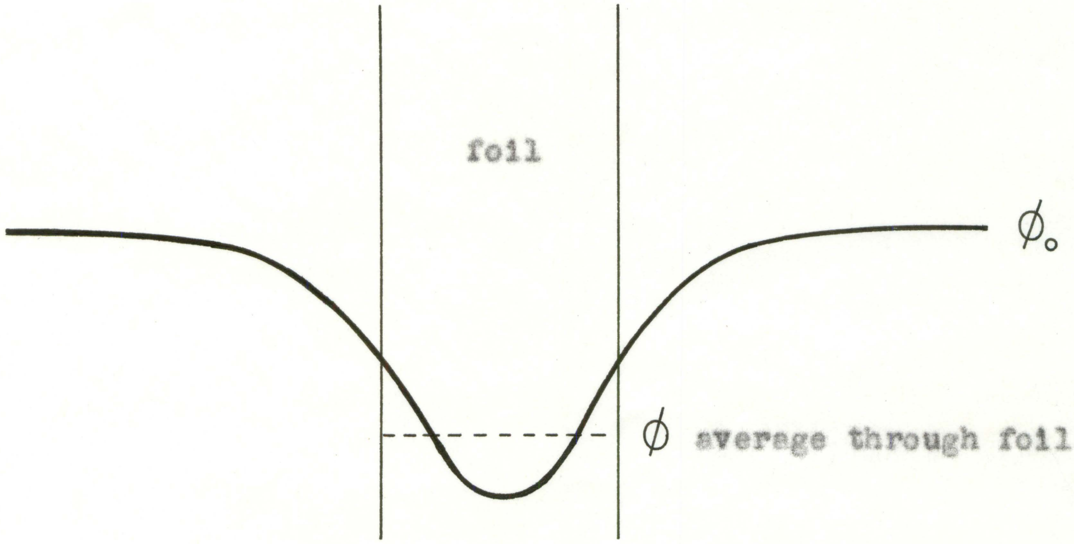

(b) Total flux-perturbation due to self-shielding plus flux depression in the surrounding medium

Figure 1. Schematic of flux perturbation in a detector foil

error made in G by this assumption is very small--approximately 0.5%.

Bothe's formula for the flux depression factor H was slightly modified by Tittle (10), the final result being

$$H = \frac{1}{1 + \frac{\alpha}{2}\left(\frac{3}{2}\frac{R}{\lambda_{tr}}\frac{L}{R+L} - 1\right)}$$

if $R > 2\lambda_{tr}$

or

$$H = \frac{1}{1 + 0.34\alpha\frac{R}{\lambda_{tr}}}$$

if $R \ll \lambda_{tr}$

where R = foil radius, cm

λ_{tr} = transport mean free path in medium around foil, cm

$\alpha = 1 - e^{-x}(1-x) - x^2E_1(x)$

$$L^2 = \frac{\lambda_{tr}\ \lambda_a}{3\left(1 - 2\frac{\lambda_{tr}}{\lambda_a}\right)^2}$$

λ_a = absorption mean free path in medium around foil, cm.

The perturbation factor, that is, the ratio of the average flux measured in the detector to the unperturbed flux is then

$$F = GH$$

Skyrme (7) solved the problem by transport-perturbation theory using much the same assumptions that Bothe did.

A few investigators have determined experimentally the flux perturbation factor of gold in graphite. The main objective of their experiments was to compare their results with the existing theories. Therefore, their measurements were generally made with a thermal flux of neutrons. In this thesis the variation of the perturbation factor in fluxes which are not entirely thermal were observed, since in practice measurements are not necessarily made in thermal fluxes.

One investigator, Thompson (9), made some measurements in varying neutron spectra. He used 1-cm radius indium foils in a graphite medium. The foils were irradiated in three neutron spectra; a thermal flux, and fluxes with cadmium ratios of 2.9 and 1.9. The results showed a much greater flux perturbation for the non-thermal fluxes. The flux having the lower cadmium ratio (relatively less thermal neutrons) had the greater perturbation. However, Thompson's results do not show any real significance, because he does not separate the thermal flux from the epi-cadmium flux. A flux measured at the lower cadmium ratio will normally contain a larger proportion of resonance neutrons than a flux measured at a higher cadmium ratio. The resonance cross section for gold is 1558 barns while the thermal cross section is 98 barns. Therefore, the rate of absorption of the resonance neutrons will be greater than the rate of absorption of thermal neutrons. (See Figure 2.) The perturbation will be

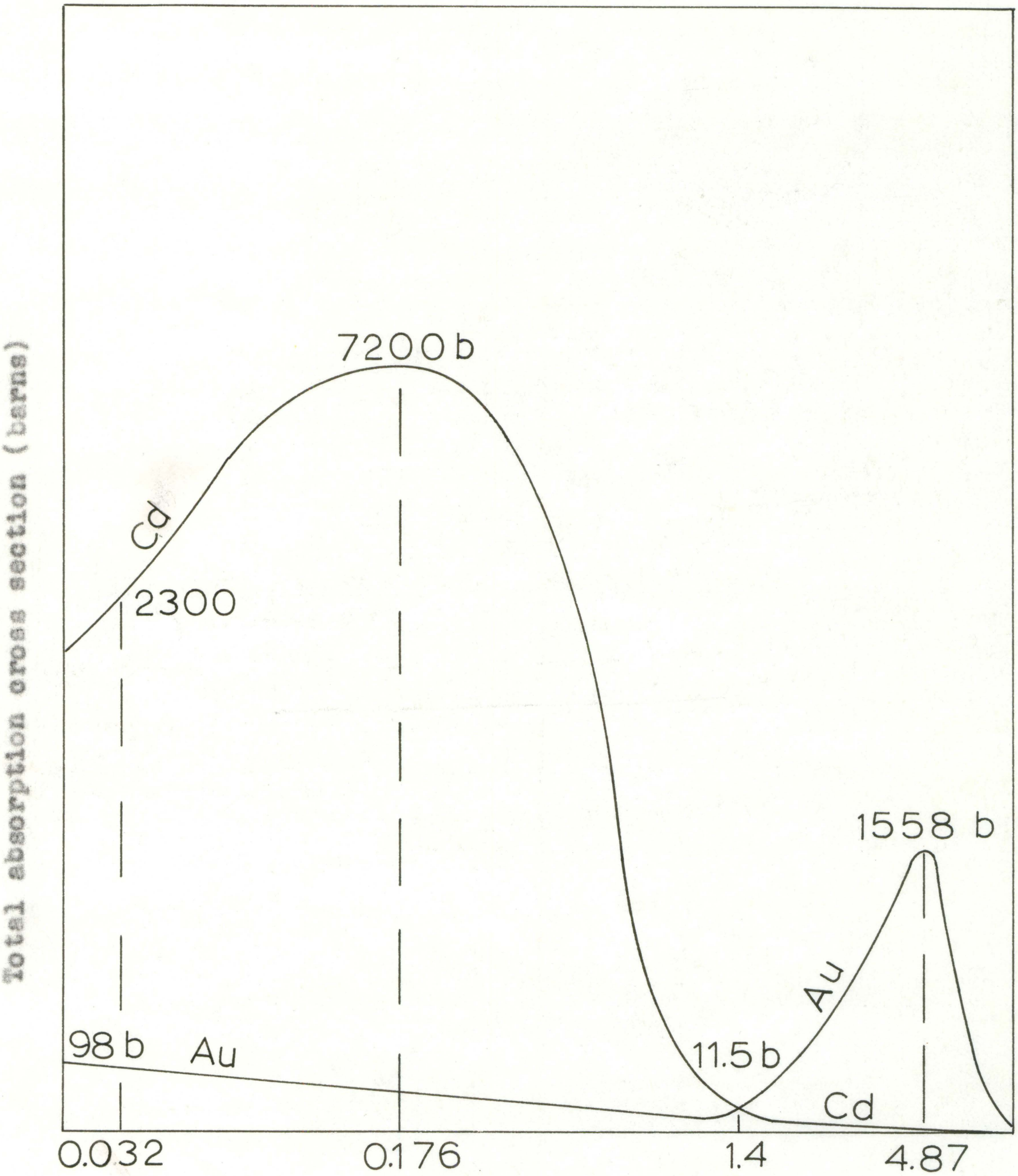

Figure 2. Absorption cross section versus neutron energy for cadmium and gold

greater in proportion to the larger number of resonance neutrons present. When a gold foil is used as a detector, it is not of any value to know the perturbation of the total flux when the flux has a wide energy distribution. It would not be known which proportion of the perturbation was due to the depression of the thermal flux and which was due to the depression of the resonance flux.

A more logical approach to the problem is to determine the perturbation of only the thermal portion of the flux as the cadmium ratio changes.

III. THEORY OF FLUX PERTURBATION IN FOILS

Since the depression of the flux is caused by the absorption of neutrons, any variable which causes a change in the absorption of neutrons should also cause a change in the perturbation factor. However, since the perturbation factor is a ratio, a change in the number of neutrons absorbed would not necessarily cause a change in the perturbation factor. For example, if the number of neutrons absorbed by the foil was doubled by doubling the flux acting on the detector, the perturbation of the flux by the foil should also be doubled. The perturbation factor would remain unchanged.

Now if the thickness of the foil is doubled, approximately[1] twice as many neutrons will be absorbed by the foil, causing an increase in the perturbation of the flux. In this case the flux in the surrounding medium was not changed (except near the foil). Therefore, the perturbation factor was decreased.

It has been established that the thickness of a thin circular (or square) detector foil greatly effects the flux perturbation factor. Under specific conditions the amount of change in the perturbation factor for change in foil thickness

---

[1]Not quite twice as many since flux perturbation will cause a reduction of the flux in the foil.

has been established within a few per cent.[2] To obtain agreement with these previous results specific conditions must be met. Some of these conditions for the experimental measurement are the following:

1. Use of a thin foil applicable to neutron detection.

2. Isotropic flux in a diffusion medium.

3. Almost entirely thermal flux (cadmium ratio over 100).

The first condition is relatively easy to accomplish. There are a number of detector materials which can be used; e.g., gold, indium, dysprosium, and aluminum. From the standpoint of available information on flux perturbation gold and indium are the best detector materials.

It is difficult to create a purely isotropic flux. However, the assumption of an isotropic flux in the center of the thermal column of the reactor will give a good approximation.

Although an almost entirely thermal flux can easily be accomplished, this is not always the condition under which a desired measurement of the flux will be made. For example, a flux measured near the core of the reactor is not made in thermal flux.

When a neutron flux with a wide energy distribution is measured, the thermal portion of the flux is often of greatest

---

[2]See chart by Sola, Table 1.

importance in measuring the magnitude of the flux. This thermal portion of the flux is measured by the cadmium difference method. A cadmium covered foil as well as a bare foil are exposed to the flux. The cadmium cover absorbs all of the thermal neutrons allowing the foil to be activated by those epicadmium neutrons which fall in the resonance range of the absorber foil. The activity of a cadmium-covered foil is subtracted from the bare foil (total) activity leaving the thermal activity. Since the cadmium cover is not a perfect absorber of thermal neutrons, some leak through to activate the cadmium covered foil. The correction to give the true thermal activation is made by the cadmium correction factor, F_{Cd}.

$$F_{Cd} = \frac{\text{Activation due to epicadmium neutrons}}{\text{Actual activation of Cd-covered foil}}$$

The purpose of this experiment is to determine whether or not flux perturbation factors measured or derived in or for entirely thermal fluxes can be applied to the thermal portion of a flux having a wide energy distribution.

The following theory is developed in Meghreblian and Holmes (4). In order to calculate what the perturbation factor should be for a detector foil in a thermal flux a model is chosen which resembles the physical situation. First, the assumption is made that the absorber foil is in an isotropic neutron flux field.

Two different models which allow relatively easy calculation are available from diffusion theory.

1) In the <u>diffusion model</u> the neutron is assumed to make many scattering collisions within the foil before it is absorbed or it escapes. It can be seen that for a strong absorber of thermal neutrons such as gold the neutron would <u>not</u> tend to be scattered many times on the average before it is absorbed or it escapes from the thin foil. Through calculations the author found that the diffusion model did not apply.

2) In the <u>first-flight transport model</u> the neutron makes no scattering collisions in the foil, but continues along a straight line until it escapes or suffers an absorption collision.

<u>Definition of terms</u>

The transmission coefficient, α.

$\alpha \equiv$ fraction of all neutrons incident upon the surface of absorbing foil of material which pass through the foil without being absorbed.

Flux perturbation factor, Fth.

$$F_{th} = \frac{\text{Average flux throughout volume of an absorber}}{\text{Value of flux at position of absorber before it was introduced}}$$

The general procedure for solving the first-flight transport model is first to solve for the transmission coefficient which is related to the flux perturbation factor.

The complete directional specification of the current is

$$j(\mu, \psi)\, d\mu\, d\psi = \frac{1}{4\pi} \phi_o \mu\, d\mu\, d\psi \qquad (1)$$

where ϕ_o = magnitude of the isotropic flux

μ = cos θ.

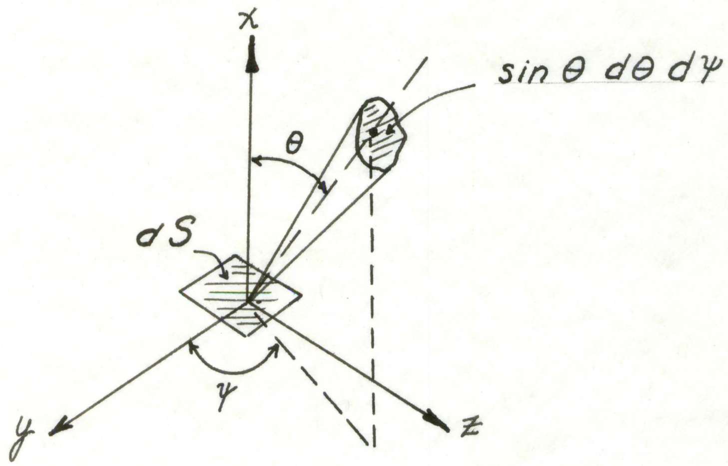

Figure 3. Scatterings from direction (θ, ψ)

This expression is consistent with the angular distribution specified by an isotropic flux. The integral of equation (1) from all directions toward the foil is 1/4 $S_L \phi_o$, where S_L is the surface area of the foil.

The probability that a neutron will pass through a distance S of the foil is exp(-Σ_as). Therefore, the transmission coefficient is

$$\alpha = \frac{4}{S_L \phi_o} \int_{S_L} dS(R) \int_o^1 d\mu \int_o^{2\pi} J(\mu, \psi) e^{-\Sigma_a s(R, \mu, \psi)} d\psi \tag{2}$$

$$= \frac{1}{\pi S_L} \int_{S_L} dS(R) \int_o^1 \mu \, d\mu \int_o^{2\pi} e^{-\Sigma_a s(R, \mu, \psi)} d\psi \tag{3}$$

where dS(R) is the surface element at surface coordinate R and $s(R, \mu, \psi)$ is the straight-line distance across the foil for a neutron incident at R traveling in direction (μ, ψ). In this case, s does not depend upon the position R on the surface (except near the edges), so $s(R, \theta, \psi) \rightarrow (\theta, \psi)$, and equation (3) reduces to

$$\alpha = \frac{1}{\pi} \int_o^{\pi/2} \sin\theta \cos\theta \, d\theta \int_o^{2\pi} e^{-\Sigma_a s(\theta, \psi)} d\psi \tag{4}$$

upon integration for an infinite slab

$$\alpha = e^{-x_o} - x_o e^{-x_o} + x_o^2 E_1(x_o) \tag{5}$$

where $x_o \equiv 2 \Sigma_a a$.

The transmission coefficient is related to the flux perturbation factor, F

$$1 - \alpha = \frac{2 \Sigma_a V_L}{S_L} F = \Sigma_a \bar{s} F \tag{6}$$

where $\bar{s} = \frac{2V_L}{S_L}$

$$= \frac{4a \, S_L}{S_L} = 4a \text{ for infinite slab.}$$

$$F = \frac{1 - \alpha}{\Sigma_a \; \bar{s}} \qquad (7)$$

$$F = \frac{1 - \alpha}{2x_o} \qquad (8)$$

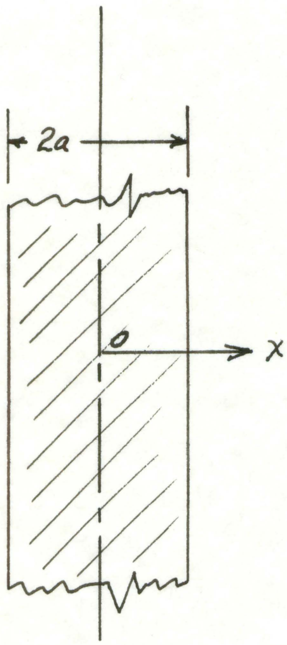

Figure 4. Cross section of infinite slab

Equation (8) was used to calculate the flux perturbation in the gold foils. The results are given in Table 3, page 36, under first flight transport approximation.

IV. EXPERIMENTAL PROCEDURE AND DESCRIPTION OF EQUIPMENT

Gold was selected as the neutron detector material for a number of reasons:

1. Gold in nature has only one isotope -- 100% Au^{197}.
2. It has a prominent absorption resonance at 4.87 ev.
3. The thermal cross section is 98 barns and has a 1/v variation.
4. The half-life of Au^{198} is 2.7 days which allows sufficient time for removal from the thermal column of the reactor and the counting of a large number of foils without appreciable decay.
5. The decay scheme of Au^{198} is very simple, with 98.7% of the beta decay accompanied by a single energy gamma ray of 411.8-kev.
6. Gold is an easy material to work for punching and weighing in the form of thin foils.

Gamma counting was desirable because the self absorption of the gamma rays by the foils would not be very great.

Graphite was an appropriate material for the surrounding medium, since it is commonly used in reactor work. In addition some experimental data of the perturbation of thermal fluxes by gold foils in graphite were available for comparison.

The general method used in measuring the perturbation factor was to irradiate stacks of identical gold foils in the reactor. The number of foils in the stack was varied from one to twelve. It had been determined by other experimenters (8-12) that a stack of foils produced exactly the same effect as a foil equal to the total stack thickness. Since it was not possible to irradiate a foil of zero thickness, it was necessary to extrapolate to zero thickness the values of activity obtained with small foil thicknesses. The corrected activities, A_{std}, obtained for the stacks of foils were directly proportional to the average flux through the stack. These activities were expressed as A_1, A_2, A_4, A_8, and A_{12}. The subscript indicated the number of foils in the stack. These relative fluxes were expressed as inverted fractions of A_{12}.

$$\frac{A_{12}}{A_8}, \frac{A_{12}}{A_4}, \frac{A_{12}}{A_2}, \frac{A_{12}}{A_1}$$

The only reason for normalizing these fluxes to A_{12} was to relate all the fluxes for the different positions to the same scale. The above fractions $\frac{A_{12}}{A_1}$, $\frac{A_{12}}{A_2}$, ... were plotted versus stack thickness. (See Figures 10-13.) This plot was then extrapolated to zero foil thickness where the fraction was $\frac{A_{12}}{A_o}$. This value $\frac{A_{12}}{A_o}$ was divided into A_{12} giving A_o. Then by definition,

$$F_i = \frac{\phi_i}{\phi_o} = \frac{A_i}{A_o}$$

the perturbation factors could be calculated.

Since it was desired to measure the flux perturbation in gold over a range of cadmium ratios, four positions were selected along the central stringer of the graphite thermal column in the UTR-10 reactor. The central stringer of the thermal column was chosen in an attempt to obtain a symmetrical flux across the line of foils. These four positions were all in a direct line, but as widely spaced as possible. (See Figure 5.) This spacing of about 24 inches between positions allowed foils to be irradiated at all four positions during a single reactor run without causing significant interaction between the foils. According to Thompson (9) there was some slight interaction between indium foils that were spaced as far as 10 inches apart within an anisotropic flux equivalent to 6 per cent change in flux per centimeter along the line of centers.

For each run a standard bare gold foil was placed in the stringers 12 inches to each side of the central stringer. These standards were used to measure the variations in reactor power from one irradiation to the next.

To determine the cadmium ratio at each of the four positions, a single bare gold foil was irradiated in each location. Then a single foil covered with a 0.020 inch cadmium cover was irradiated at each position. The ratio of the activity of a bare foil to the activity of a cadmium-covered foil gave the cadmium ratio at each position. These cadmium

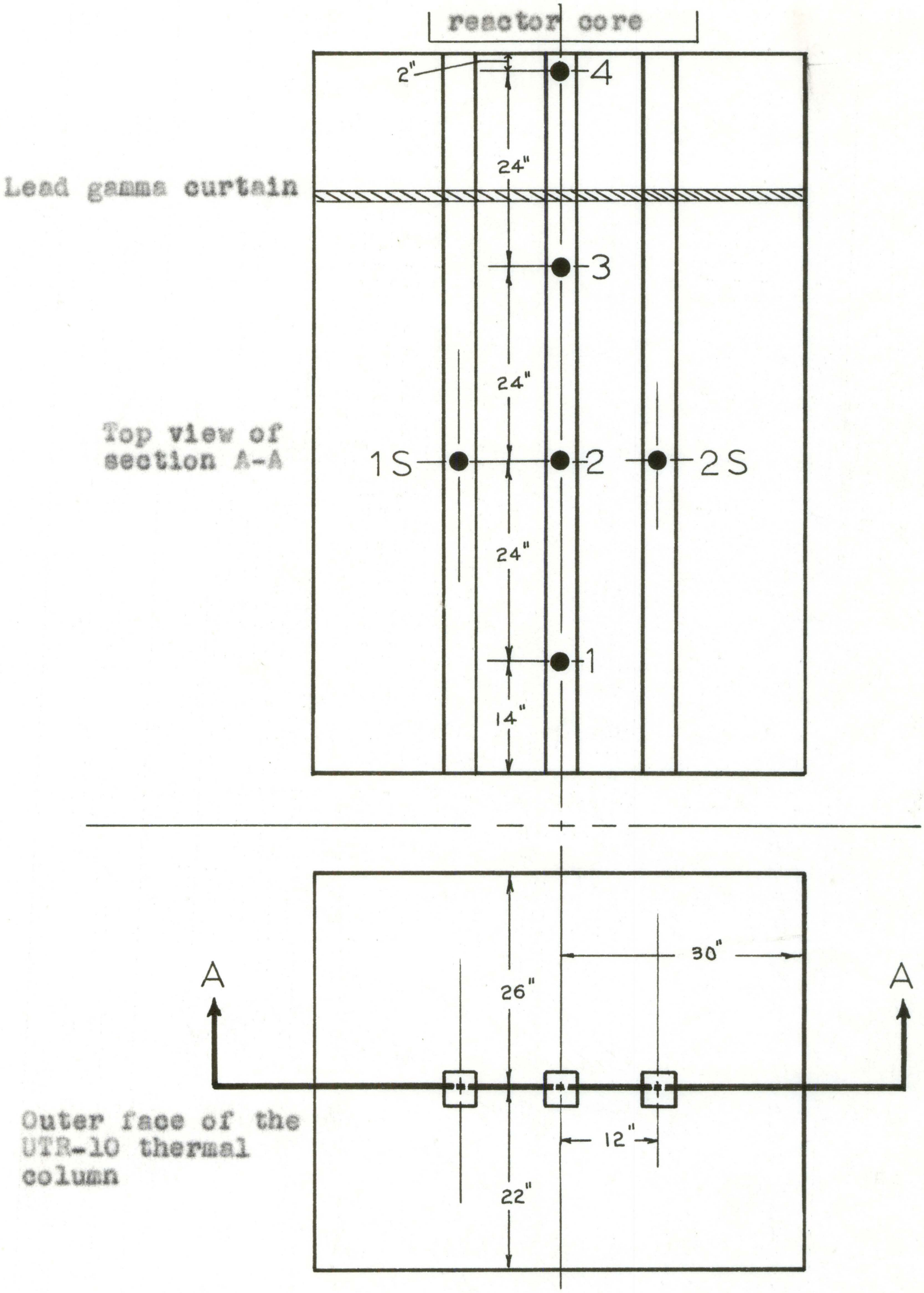

Figure 5. Locations of gold foils in the UTR-10 thermal column

ratios were corrected with a cadmium correction factor which took into account the fact that the cadmium cover was not a perfect filter, but allowed some of the thermal neutrons to leak through. Tittle (10) had stated that a 0.020 inch cadmium cover would absorb all of the thermal neutrons. Therefore, the experiment was performed using 0.020 inch cadmium covers. However, subsequent measurement of the cadmium correction factor showed that a 0.020 inch thick cadmium cover was not black (totally absorbant to thermal neutrons). The cadmium correction factor was determined experimentally by using cadmium covers with thicknesses varying from 0.010 inch up to 0.080 inch.

Gamma counting was accomplished with a NaI(Tl) crystal coupled to a photomultiplier tube with the pulse amplified and fed into a Model 181A Nuclear Chicago Scalar with a fixed sensitivity setting of 50 mv. The crystal was covered with an aluminum cap to absorb the beta particles. The activated gold foils were placed in a lead shield which was partially surrounded by another 2 inches of lead since the background gamma was quite high in the counting room. The background count was reduced from 10,000 counts per minute to 300 counts per minute by the lead shielding.

The gold foils were all circular, 1/2 inch in diameter, and 0.001 inch thick. They were punched out; then they were weighed to ± 0.1 mg. The approximate weight was 60 mg.

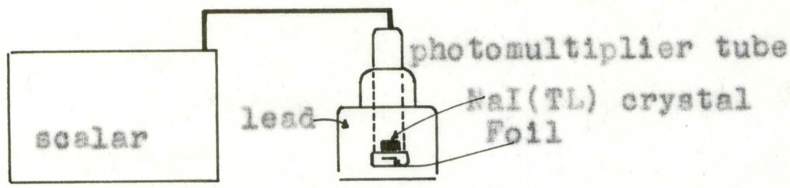

Figure 6. Counting set up

The cadmium covers were punched from sheets of cadmium and formed into cups which fitted inside of each other. All cadmium covers except those used to determine the cadmium correction factor were 0.020 inch thick. (See Figure 7a.)

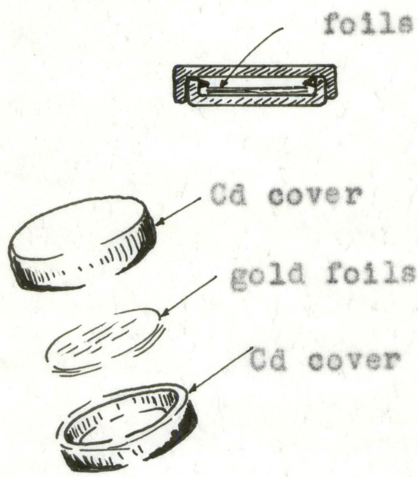

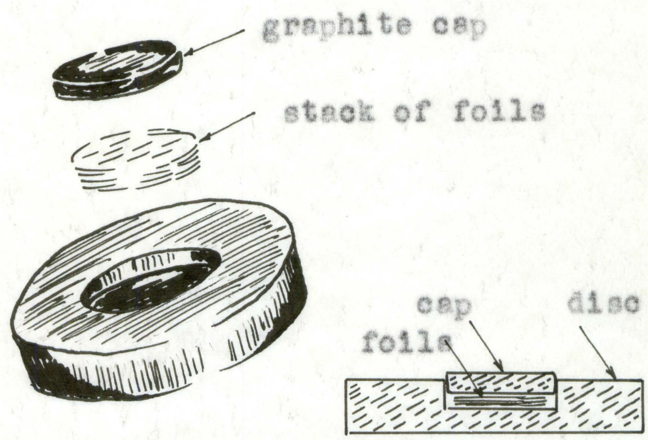

Figure 7a. Cadmium cover Figure 7b. Graphite disc

The bare gold foils that were placed in the reactor were stacked in graphite discs. Each graphite disc had a small depression in the top which was just large enough to allow a 1/2 inch diameter gold foil to be stacked in it. The stack of foils was pressed down in the depression in the graphite disc by means of a small graphite cap. (See Figure 7b.) This procedure insured the straight alignment of the stack and tight packing of the foils on top of each other. The cadmium covered foils were not placed in graphite discs.

To determine the flux perturbation factor bare gold foils were activated and their activity counted for the four positions along the central stringer of the reactor thermal column. Stack thicknesses of 1, 2, 4, 8, and 12 mils were used. Then cadmium-covered gold foils were activated and counted for positions 3 and 4. These positions were the ones closer to the reactor core and at the lower cadmium ratios. The flux at the other two positions (1 and 2) giving cadmium ratios of 1534 and 125 was considered to be essentially thermal. Therefore, the bare foil activities were sufficient to measure the thermal fluxes at positions 1 and 2. Cadmium-covered stack thicknesses of 1, 2, 4, 8, and 12 mils were again used.

The cadmium correction factor was determined by activating 1-mil-thick gold foils at position 3 using cadmium cover thicknesses of 10, 20, 30, 40, 50, 60, and 80 mils. These activities versus the cadmium cover thickness were then plotted. (See Figure 8.) The straight line portion of the plot represents the attenuation of epicadmium neutrons by the cadmium. The curved portion shows the leakage of thermal

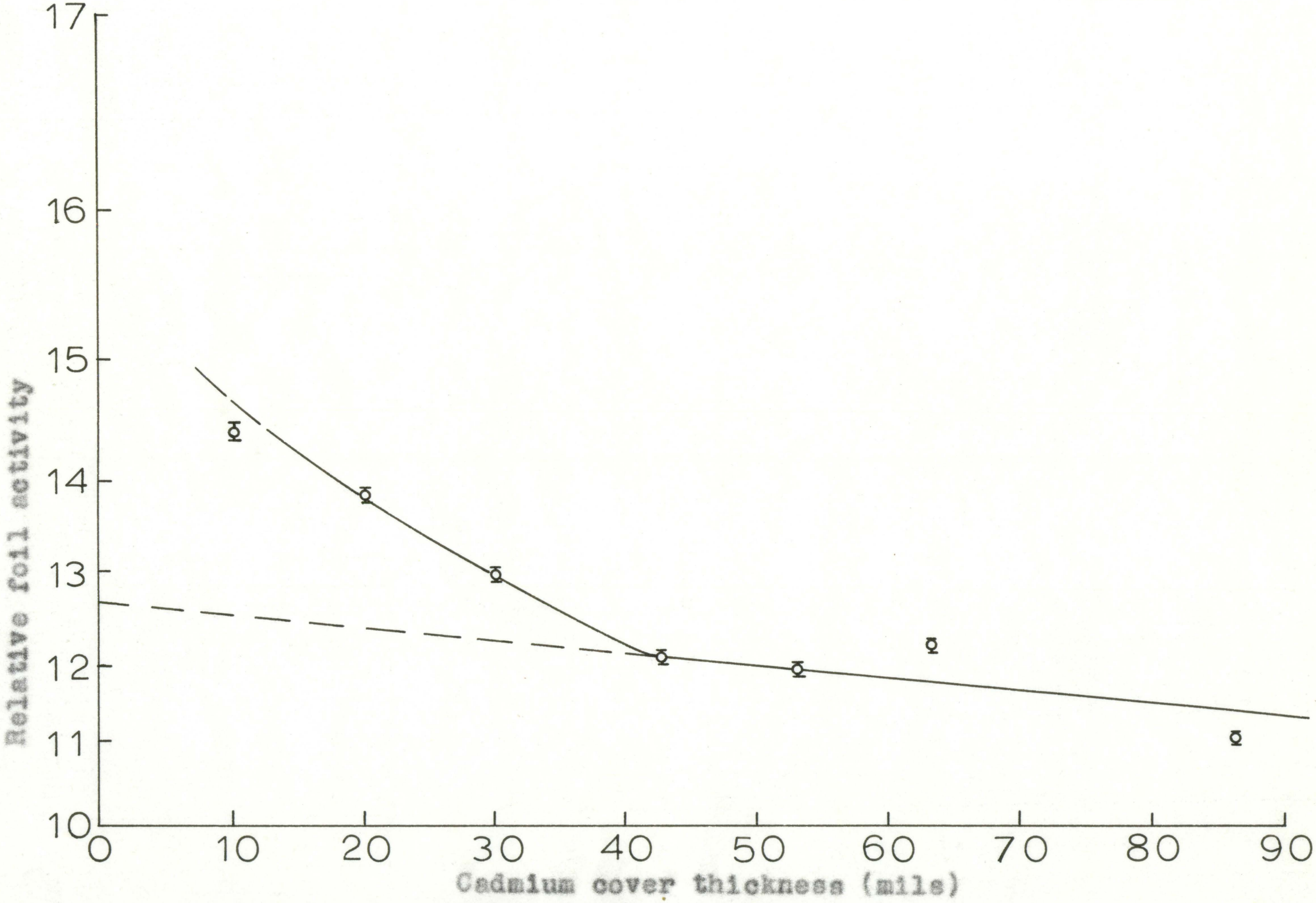

Figure 8. Relative foil activity versus cadmium cover thickness

Table 2. Cadmium correction factor data

Cadmium thickness (mils)	Corrected foil activity (relative)
10	14.56
20	13.81
30	12.93
40	12.05
50	11.93
60	12.17
80	11.29

neutrons through the cadmium cover. The straight line portion of the graph was extrapolated back to zero cadmium thickness. This activity represented the activation of the gold foil that would have resulted if all of the epicadmium neutrons had passed through the cadmium, but none of the thermal neutrons had penetrated the cadmium to activate the gold. This activity at zero cadmium thickness was divided by the activity at 20 mil cadmium thickness to give the cadmium correction factor to be applied to cadmium ratios measured with 20 mil cadmium covers.

In measuring the activities of all foils throughout the experiment the following corrections were applied to the counting rates in the following order:

1. Dead time
2. Background
3. Variation in foil weight
4. Foil decay time
5. Variation in reactor power.

The data for the above corrections are shown in Table 6 in the Appendix.

Dead time correction

The dead time, 5 μ seconds, of the scalar was the determining factor in counting system, since the resolving time of the NaI(Tl) crystal and photomultiplier tube was much shorter, about 0.25 μ second. The number of counts lost by the scalar increased linearly as the counting rate increased.

r_d = true count/minute

r = observed count/minute

τ = dead time-minutes

$$r_d = \frac{r}{1 - r\tau}$$

$$r_d = \frac{(47{,}062\ c/m)^{*}(60\ sec/min)}{1 - (47{,}062\ c/m)(5 \times 10^{-6}\ sec)}$$

$$r_d = 47{,}248\ c/m$$

---

*Counting rate for foil 3CdM1.

Background correction

r_{-b} = counting rate corrected for background

r_d = counting rate before background correction

r_b = background counting rate

$$r_{-b} = r_d - r_b$$

$$r_{-b} = (47{,}248 - 355)\text{c/m}$$

$$r_{-b} = 46{,}893 \text{ c/m}$$

Normalizing for foil weight

r_{-b} = counting rate before normalizing for foil weight

r_n = counting rate after normalizing for foil weight

Wgt = foil weight

$$r_n = \frac{r_{-b}}{\text{Wgt}}$$

$$= \frac{46{,}893 \text{ c/m}}{0.0613 \text{ gm}}$$

$$= 765{,}000 \text{ c/m gm}$$

$$= 765.0 \text{ c/m mg}$$

Foil decay correction

All foils were irradiated at constant power for 20 minutes. However, the period of constant power was preceded by a period of increasing reactor power during start up and followed by a period of decreasing reactor power during shut down or scram. The start up time during which the reactor was at a sufficient power level to effect the activation of the foil was short (approximately 2 minutes) in comparison with the constant power run (20 minutes). The scram time was much shorter (a few seconds). Any fluctuations in the integrated power from one run to the next were measured by the activation of the standard foils. Therefore, it was unnecessary to apply the decay correction to the start up or shut down period. The standard decay equation was used to calculate the activity that the foil would have had if it had been irradiated to saturation and counted immediately upon removal from the flux. Making the assumption that the power dropped instantly to zero when the reactor scramed, the decay correction was applied to the period of constant power with t_w beginning at the instant of reactor scram. Exposure time, t_e, was taken as the time at constant power. The standard decay equation is

$$A_{(x)} = \frac{\lambda M_e^{\lambda t_w}}{(1-e^{-\lambda t_e})(1-e^{-\lambda t_c})}$$

where $A_{(x)}$ = saturation activity at time of removal

M = counts/mg.

λ = $1.7824\ (10)^{-4}\ \text{min}^{-1}$, decay constant for gold

t_e = time of exposure (min)

t_c = time of count (min)

t_w = time of wait (min) from scram to start of count

r_n = normalized counting rate (c/m).

For t_e and $t_c \leq 23$ min.

$$(1-e^{-\lambda t_e}) \simeq \lambda t_e$$

$$\text{and } (1-e^{-\ t_c}) \simeq \lambda t_c$$

Therefore

$$A(x) = \frac{\lambda(r_n)(t_c)e^{\lambda t_w}}{\lambda t_e \lambda t_c}$$

which reduces to

$$\frac{r_n\ e^{\lambda t_w}}{t_e\ \lambda}$$

$$= \frac{r_n\ e^{\lambda t_w}}{(20)(1.7824)(10)^{-4}} \qquad \text{for } t_e = 20 \text{ min}$$

$$= 280\ r_n\ e^{(1.7824\ \text{min}^{-1})(t_w)}$$

$$= 280\ (765.0)\ e^{(1.7824)(358)}$$

$$= 815.5\ (280)\ \text{c/m-mg}$$

The constant 280 was dropped since all fluxes were relative.

Reactor power normalization

The reactor power of run D was chosen as the base level to which all other runs were normalized.

Corrections for variations in reactor power from one run to the next were made by relating the activity of the standard foils of each run to the standard foils of run D.

A_{std} = foil activity normalized (standardized) to run D

$A_{(x)}$ = foil activity before normalizing for power level

$$A_{std} = \frac{(\text{Average } A_{(x)} \text{ of standards from run D})(A_{(x)} \text{ of particular foil})}{\text{Average } A_{(x)} \text{ of standards from particular run}}$$

$$= \frac{(1762 \text{ c/m-mg})(815.5 \text{ c/m-mg})}{(1684.5 \text{ c/m-mg})}$$

$$= 850.4 \text{ c/m-mg}$$

After a stack of foils was irradiated, the activity of each of the individual foils in the stack was measured. Corrections 1 through 4 were made to that activity. Then the corrected activities of all the foils in a single stack were used to determine the average activity across the stack. Measuring the activities of the individual foils in the stack eliminated the need for corrections due to changes in geometry which varying stacks of foils under the crystal would have required. It also made it unnecessary to make corrections for the absorption of the gamma rays by the succeeding layers of foils.

The standard deviations calculated by counting statistics were less than 0.75% for all data used in the determination of the flux perturbation factors and the cadmium correction factor.

The estimated standard deviation of the weight of the foils was 0.33%($\pm$ 0.1 mg for a 60 mg foil).

The total accumulated percentage error from counting statistics and foil weight was approximately 1%.

V. EXPERIMENTAL AND THEORETICAL RESULTS

The relative average saturation activities through the stacks of foils after all corrections were made are shown in Table 4.

The corrected activities obtained with cadmium cover thicknesses of 10 to 80 mils are shown in Table 2. These activities are plotted in Figure 8. The cadmium correction factor was calculated to be 0.912.

The measured flux perturbation factors are shown in Table 3 along with the values calculated using the first flight transport approximation. Figure 9 shows a plot of the measured flux perturbation factors and those calculated from the first flight transport approximation versus foil stack thickness.

The perturbation factor is seen to become less in all cases as the cadmium ratio at which the measurements were made decreases. The perturbation factors measured in the foils at positions 3 and 4 (cadmium ratios 7.9 and 4.1 respectively) are seen to be considerably lower than the perturbation factors measured at the thermal positions 1 and 2 (cadmium ratios 1534 and 125 respectively). Also the perturbation factors measured at positions 3 and 4 are close to the values calculated using the first flight transport model.

The experimental values by Sola and the theoretical

Table 3. Flux perturbation for circular gold foils in graphite

	Foil thickness in mils				
	1	2	4	8	12
Position 1 C.R.=1534 Measured	0.996	0.990	0.975	0.886	0.802
Position 2 C.R.=125 Measured	0.991	0.967	0.938	0.873	0.793
Position 3 C.R.=7.91 Measured (thermal)	0.954	0.905	0.870	0.805	0.765
Position 4 C.R.=4.14 Measured (thermal)	0.951	0.885	0.844	0.789	0.759
First-flight transport approximation	0.963	0.934	0.881	0.801	0.759

values of Bothe and Skyrme are also close to those obtained at positions 3 and 4.

The values calculated using the first-flight transport model and based on diffusion theory are almost identical with the calculated results of Skyrme who uses equations based on transport theory. Skyrme's formula takes into account the radius of the foil and the properties of the diffusion media surrounding the foil.

The perturbation factors obtained for positions 1 and 2 are somewhat high and the curves of perturbation factor versus stack thickness have a different slope than might be expected. The curves are convex instead of concave.

Table 4. Relative average saturation activities for stacks of gold foils

	Foil thicknesses (in mils)				
	1	2	4	8	12
Position 1					
Bare activity	220.4	219.0	215.7	195.6	177.1
Cd-covered act.	0.130				
Position 2					
Bare activity	2150	2097	2038	1891	1720
Cd-covered act.	15.7				
Position 3					
Bare activity	11,894	11,020	10,398	9,512	8,900
Cd-covered act.	1,371	1,008	752.6	582.9	496.6
Position 4					
Bare activity	34,574	30,900	28,576	26,111	24,750
Cd-covered act.	7,623	5,765	4,532	3,517	2,996

Table 5. Calculated data

Position 1

Stack thickness (mils)	Bare activity	$\frac{\phi_{12}}{\phi_1}$	Fth.
1	220.4	0.805	0.996
2	219.0	0.810	0.990
4	215.7	0.822	0.975
8	195.6	0.906	0.886
12	177.1	1.000	0.802

Position 2

Stack thickness (mils)	Bare activity	$\frac{\phi_{12}}{\phi_1}$	Fth.
1	2150	0.800	0.991
2	2097	0.820	0.967
4	2038	0.845	0.938
8	1891	0.909	0.873
12	1720	1.000	0.793

Position 3

Stack thickness (mils)	Bare activity	(Cd-covered activity) (F_{Cd})	Thermal activity	$\frac{\phi_{12}}{\phi_1}$	Fth.
1	11,894	1251	10,643	0.803	0.954
2	11,020	918	10,102	0.846	0.905
4	10,398	686	9,712	0.880	0.870
8	9,512	531	8,981	0.951	0.805
12	8,900	453	8,547	1.000	0.765

Position 4

Stack thickness (mils)	Bare activity	(Cd-covered activity) (F_{Cd})	Thermal activity	$\frac{\phi_{12}}{\phi_1}$	Fth.
1	34,574	6950	27,624	0.797	0.951
2	30,900	5260	25,740	0.859	0.885
4	28,576	4130	24,446	0.900	0.844
8	26,111	3204	22,907	0.962	0.789
12	24,750	2732	22,018	1.000	0.759

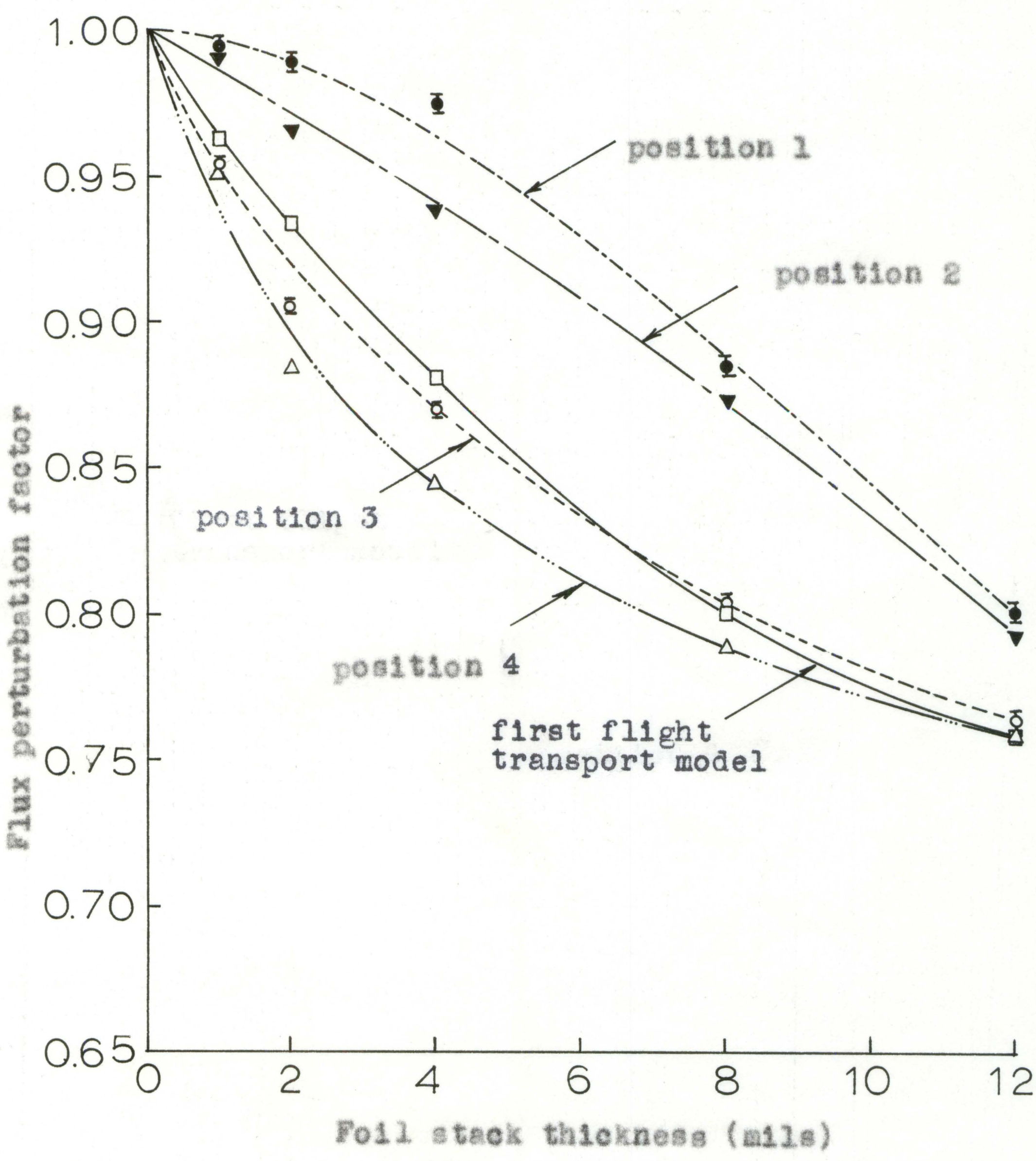

Figure 9. Flux perturbation factor versus foil stack thickness

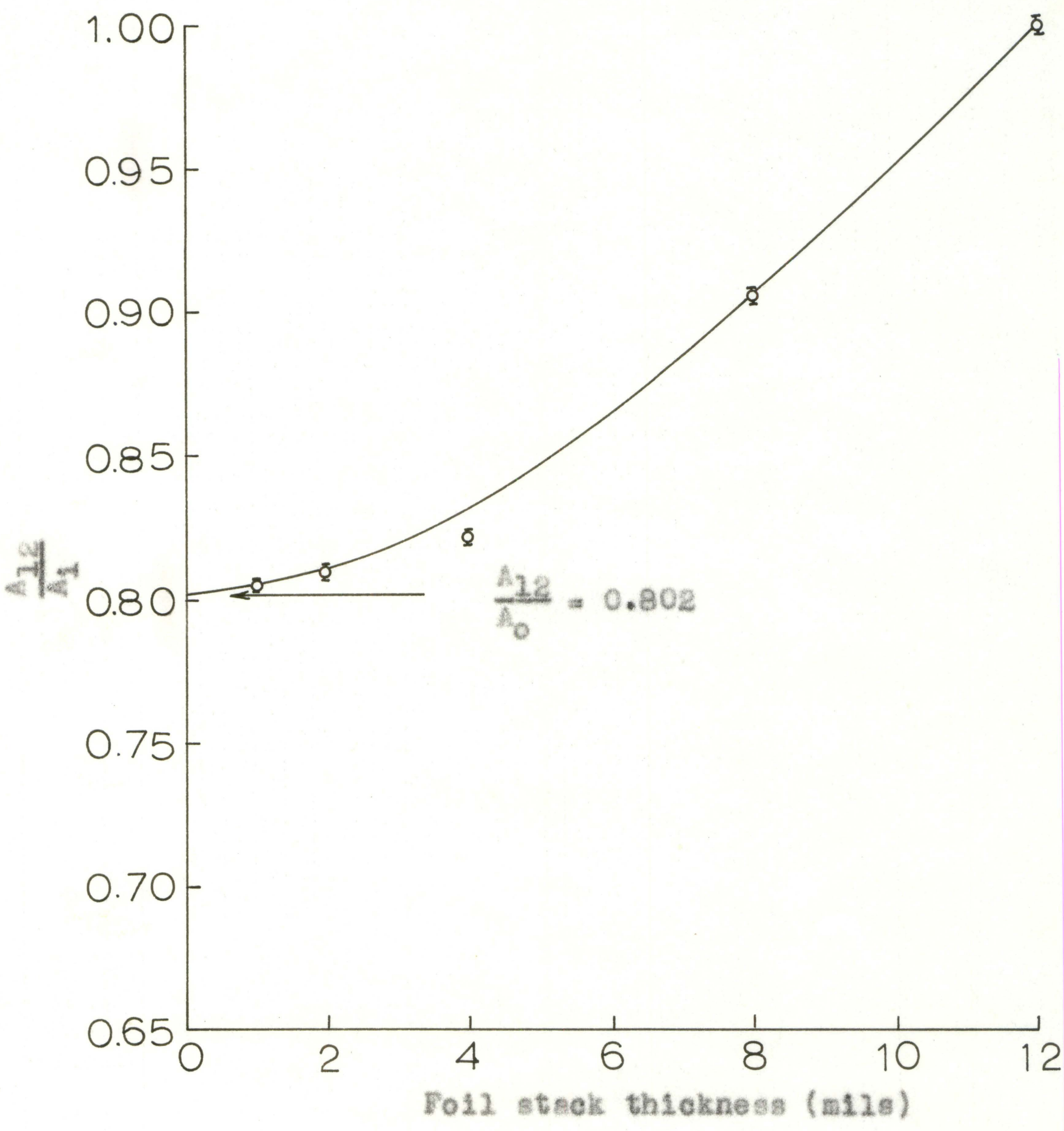

Figure 10. Extrapolation to zero thickness absorber for position 1

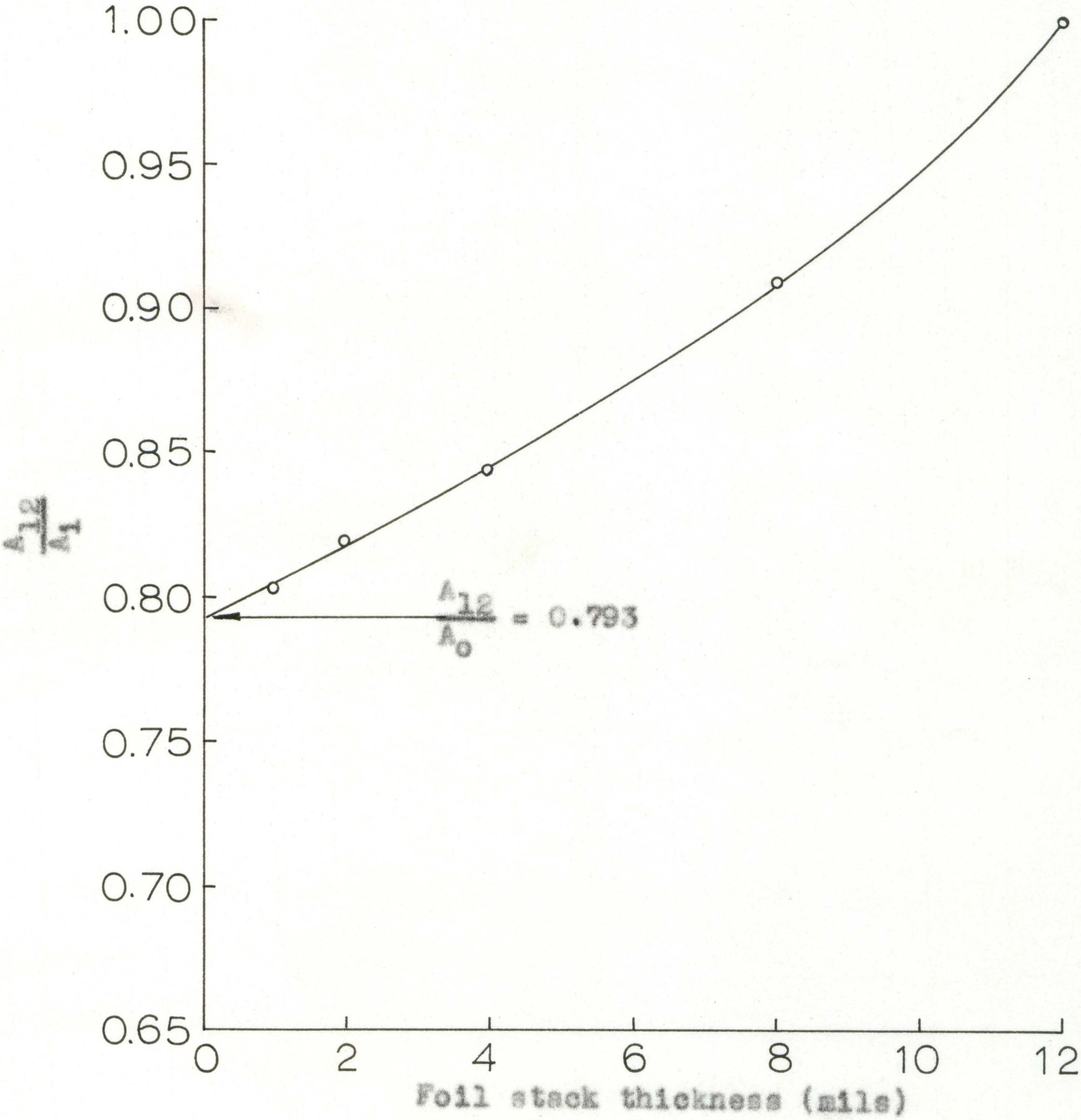

Figure 11. Extrapolation to zero thickness absorber for position 2

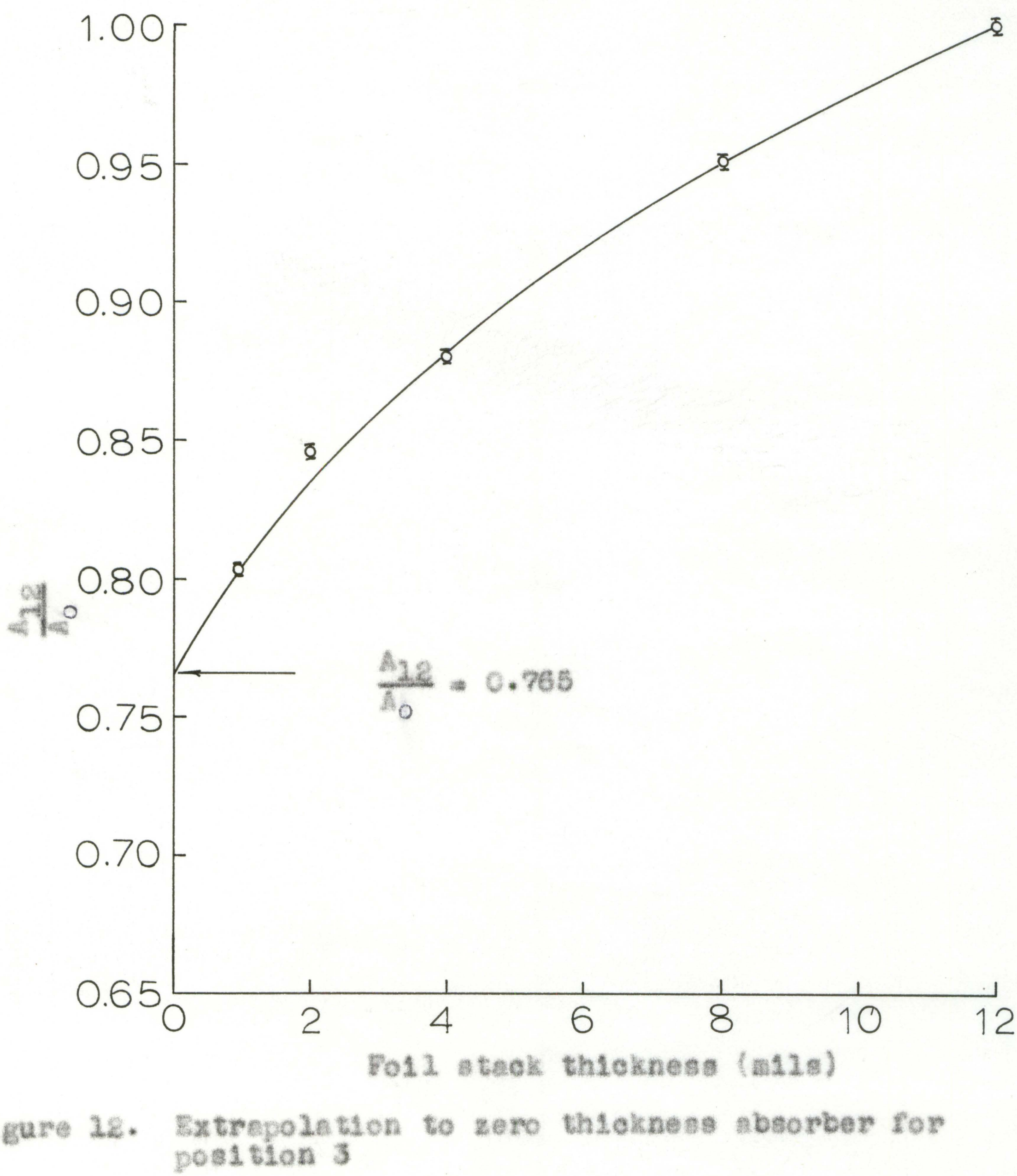

Figure 12. Extrapolation to zero thickness absorber for position 3

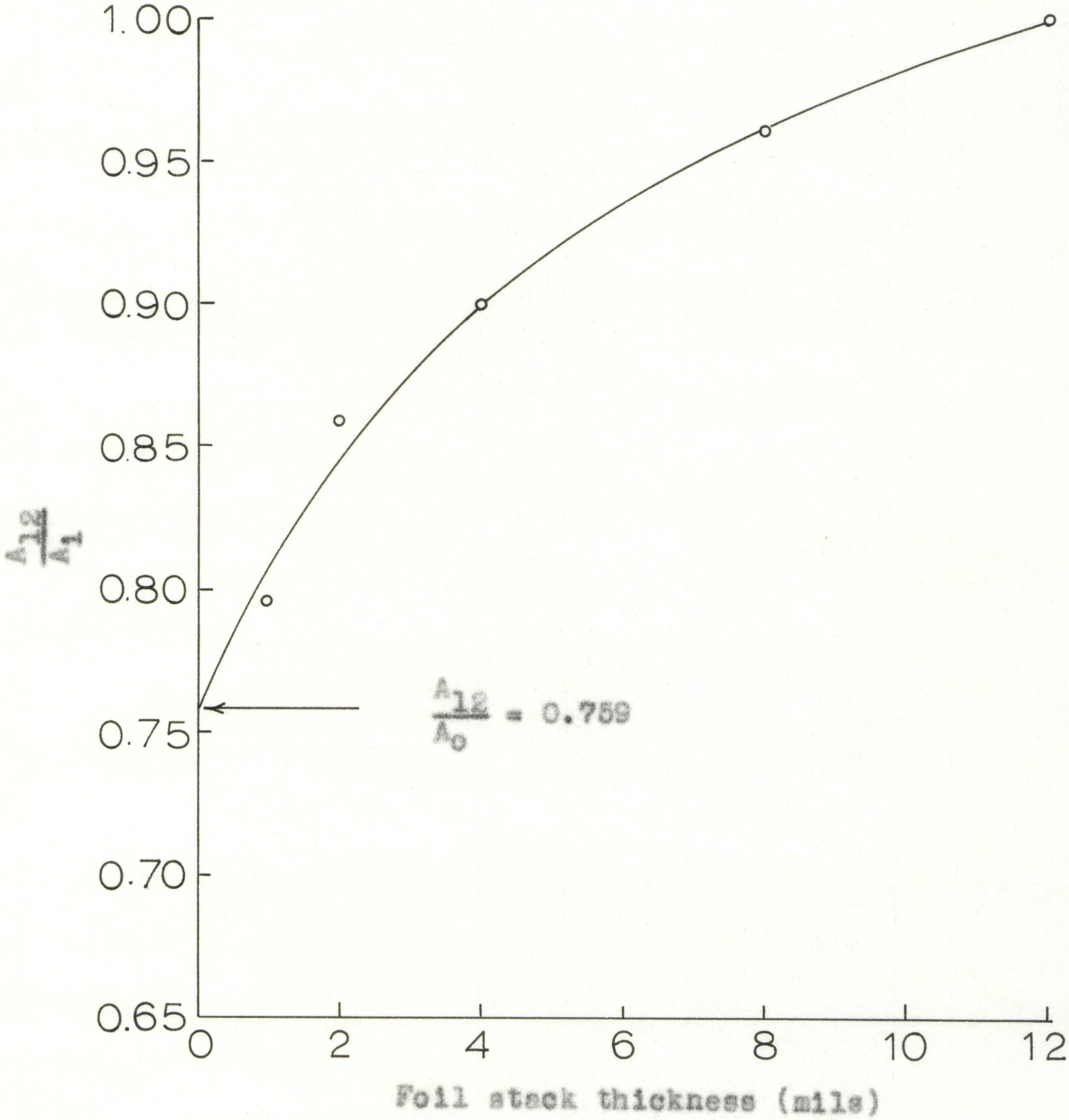

Figure 13. Extrapolation to zero thickness absorber for position 4

VI. CONCLUSIONS

The perturbation of the thermal portion of the flux by gold foils in regions of low cadmium ratio was found to agree closely with the perturbation obtained by other experimenters in thermal fluxes and with the calculated theoretical values.

Therefore, it is concluded that the perturbation factors measured for thermal fluxes can be applied to the thermal portion of fluxes measured at low cadmium ratios.

Since the perturbation factors in this experiment measured for fluxes in the entirely thermal region did not agree with those measured at low cadmium ratios or with the results of other experimenters or with theoretical calculations, they must have been affected by some factor other than the change in cadmium ratio.

A number of possible causes for the high perturbation factors at positions 1 and 2 were considered such as the change in angular distribution of the flux, hardening of the thermal portion of the neutron spectrum, interaction of the foils on each other, or disturbance of the flux near the boundaries of the thermal column. However, the unexpected results could not definitely be attributed to any of these possibilities. Also the difference between the slopes of the flux perturbation factor versus foil stack thickness for positions 1 and 2, and positions 3 and 4, could not be explained.

The perturbation of the flux at position 4 did not agree as closely with the results of other experimenters as the perturbation did at position 3. This was probably a result of the disturbance of the flux near the boundary of the diffusion medium. Position 4 was 2 inches from the boundary of the thermal column.

VII. RECOMMENDATIONS FOR FURTHER STUDY

In order to gain more accuracy and reliability of the experimentally determined perturbation factors additional data points could be taken. It would be particularly helpful to take data with thinner foils to make the extrapolation to zero foil thickness more reliable.

An experiment should be performed to determine whether or not the angular distribution of the flux changes for different positions in the thermal column.

Also a more accurate determination of the cadmium correction factor should be made.

The possibility of interaction between the foils should be investigated. This could be done by placing foils progressively closer to each other in the thermal column until some change in the relative activation of the foils resulted.

VIII. LITERATURE CITED

1. Bothe, W. Zur Methodik der Neutronen sonden (Concerning the methodology of neutron probes). Z. Physik 120: 437. (Original available but not translated; reviewed in Sola, A. Flux perturbation by detector foils. Nucleonics 18, No. 3: 78-81 and 141. March, 1960.)

2. Glasstone, S. and Edlund, M. C. The elements of nuclear reactor theory. Princeton, N.J., D. Van Nostrand Company, Inc. 1952.

3. Martin, D. H. Correction factors for Cd-covered foil measurements. Nucleonics 13, No. 3: 52-53. March, 1955.

4. Meghreblian, Robert V. and David K. Holmes. Reactor analysis. New York, N.Y., McGraw-Hill Book Company, Inc. 1960.

5. Price, William J. Nuclear radiation detection. New York, N.Y., McGraw-Hill Book Company, Inc. 1958.

6. Ritchie, R. H. and others. Thermal neutron flux depression. U. S. Atomic Energy Commission Report ORNL-2806 Oak Ridge National Lab., Tenn. : 133-137. July 31, 1959.

7. Skyrme, T. H. R. Reduction in neutron density caused by an absorbing disc. United Kingdom Atomic Energy Authority. MS-91. 1961.

8. Sola, A. Flux perturbation by detector foils. Nucleonics 18, No. 3: 78-81 and 141. March, 1960.

9. Thompson, M. W. Some effects of the self-absorption of neutrons in neutron-detecting foils. J. Nuclear Energy 2: 286-290. 1956.

10. Tittle, C. W. Slow-neutron detection by foils. II. Nucleonics 9, No. 1: 60-77. July, 1951.

11. Trubey, D. K., Blosser, T. V., and Estabrook, G. M. Correction factors for foil-activation measurements of neutron fluxes in water and graphite. U. S. Atomic Energy Commission Report ORNL-2842 Oak Ridge National Lab., Tenn. : 204-215. September 1, 1959.

12. Zobel, W. Determination of experimental flux depression and other corrections for gold foils exposed in water. U. S. Atomic Energy Commission Report ORNL-2842 Oak Ridge National Lab., Tenn. : 202-203. September 1, 1959.

13. ________. Experimental determination of flux depression and other corrections for gold foils exposed in water. U. S. Atomic Energy Commission Report ORNL-3016 Oak Ridge National Lab., Tenn. : 267-269. September 1, 1960.

IX. ACKNOWLEDGEMENTS

The author wishes to thank his major professor, Dr. Glenn Murphy, for his guidance and encouragement which made possible the completion of this thesis and also Mr. Richard Danofsky for his assistance on the experimental set up and procedure.

X. APPENDIX

Calculation of counting statistics

Calculate the standard deviation in counting rates:

$$r_s \pm \sigma_s = (r_t - r_b) \pm (\sigma_b^2 + \sigma_t^2)^{1/2}$$

reduces to $r_s \pm \sigma_s = (r_t - r_b) \pm \left(\frac{r_b}{t_b} + \frac{r_t}{t_t}\right)^{1/2}$

where $\sigma_b = \left(\frac{r_b}{t_b}\right)^{1/2}$

$\sigma_t = \left(\frac{r_t}{t_t}\right)^{1/2}$

r_s = net counting rate

r_t = total counting rate

r_b = background counting rate

t_t = time for total activity count

t_b = time for background count

σ_s = standard deviation of net counting rate

σ_t = standard deviation of total counting rate

σ_b = standard deviation of background counting rate.

For foil 1SE:

$$r_s \pm \sigma_s = (118{,}677 - 550 \text{ c/m}) \pm \left(\frac{550 \text{ c/m}}{10 \text{ min}} + \frac{118{,}677 \text{ c/m}}{2 \text{ min}}\right)^{1/2}$$

$$= 118{,}127 \pm 247 \text{ c/m}$$

% standard deviation = $\frac{247\,(100)}{118{,}127} = 0.209\%$

Explanation of column headings for Table 6

Foil--First number indicates position along thermal column in which foil was exposed.

S indicates foil used to monitor reactor power level.

Cd indicates foil was cadmium covered.

First letter or letters following letter S or Cd indicates reactor run.

Last number gives location of the individual foil in the stack starting with 1 on the top of the stack.

Example 1: Foil 1SH--number one standard foil, reactor run H.

Example 2: Foil 3H7--foil stack in position number 3, reactor run H, seventh foil from the top of the stack.

Example 3: Foil 4CdK12--foil stack in position number 4, foil stack cadmium-covered, reactor run K, twelfth foil from the top of the stack.

Wgt--Weight of foil, ± 0.0001 gm.

t_w--Time in minutes between shut down of the reactor to beginning of counting activity of the foil.

t_c--Length of time foil was counted.

counts--Total number of counts recorded.

rate--Counts/t_c (counts/minute of foil activity from gamma decay).

r_d--Counting rate (foil activity) corrected for dead time of counting system.

r_{-b}--r_d minus background activity.

r_n--r_{-b}/foil weight (counting rate normalized for foil weight).

$A_{(x)}$--r_n corrected for foil decay (activity corrected back to the activity the foil would have if irradiated to saturation and counted immediately upon removal from flux).

A_{std}--$A_{(x)}$ normalized to the reactor power level of Run D.

% σ_s--Per cent standard deviation, including standard deviations for background.

Note: All values for r_n are multiplied by 10^{-3}.

Table 6. Data for foil activity with corrections

Foil	Wgt (gm)	t_w (min)	t_c (min)	Counts	Rate, r (c/m)	r_d (c/m)	r_{-b} (c/m)	r_n (c/m)	$A_{(x)}$ (c/m)	A_{std}	% σ_s
				Reactor run: D April 6, 1962							
				Power level: 500 watts for 20 minutes							
				Cadmium covers: 20 mil thickness							
				Background activity: 617 c/m							
				Uranium standard: 84,514 counts/2 minutes							
1SD	0.0606	62	2	210,010	105,005	105,932	105,315	1,738	1,757		
2SD	0.0606	65	2	210,549	105,274	106,409	105,792	1,746	1,766		
Av.									1,762	1.0000	0.21
1D1	0.0642	53	5	73,116	14,623	14,633	14,016	218.3	220.4	220.4	0.37
2D1	0.0642	59	2	271,283	135,641	137,191	136,574	2,127	2,150	2,150	0.19
3CdD1	0.0639	43	3	260,879	86,960	87,595	86,978	1,361	1,371	1,371	0.20
4CdD1	0.0639	48	1	464,731	464,731	483,455	482,838	7,556	7,623	7,623	0.14

Table 6. (Continued)

Foil	Wgt (gm)	t_w (min)	t_c (min)	Counts	Rate, r (c/m)	r_d (c/m)	r_{-b} (c/m)	r_n (c/m)	$A_{(x)}$ (c/m)	A_{std}	% σ_s
				Reactor run: E April 12, 1962 Power level: 500 watts for 23 minutes Cadmium covers: 20 mil thickness Background activity: 550 c/m Uranium standard: 84,600 counts/2 minutes							
1SE	0.0658	93	2	232,794	116,397	118,677	118,127	17,952	1,825		
2SE	0.0658	96	2	234,447	117,223	119,713	119,163	18,110	1,842		
Av.									1,834	0.96074	0.16
1E1	0.0642	100	2	29,981	14,990	15,009	14,959	233.0	237.2		
1E2	0.0642	103	2	29,790	14,895	14,914	14,364	223.7	227.9		
Av.									232.5	219.0	0.41
2E1	0.0647	106	2	275,826	137,913	139,533	138,983	2,148	218.9		
2E2	0.0647	109	2	274,302	137,151	138,731	138,181	2,136	217.8		
Av.									218.3	209.7	0.11
3CdE1	0.0600	112	2	124,365	62,182	62,504	61,954	1,032	105.3		
3CdE2	0.0600	115	2	122,494	61,247	61,560	61,510	1,025	104.6		
Av.									104.9	1,008	0.28
4CdE1	0.0606	118	2	683,226	341,613	351,483	350,933	5,791	5,915		
4CdE2	0.0607	121	2	709,555	354,777	362,190	361,640	5,958	6,088		
Av.									6,001	5,765	0.12

Table 6. (Continued)

Foil	Wgt (gm)	t_w (min)	t_c (min)	Counts	Rate, r (c/m)	r_d (c/m)	r_{-b} (c/m)	r_n (c/m)	A(x) (c/m)	A_{std}	% σ_s
				Reactor run: F April 12, 1962							
				Power level: 500 watts for 20 minutes							
				Cadmium covers: 20 mil thickness							
				Background activity: 381 c/m							
				Uranium standard: 84,280 counts/2 minutes							
1SF	0.0650	50	2	216,709	108,359	109,359	108,978	1,677	1,692		
2SF	0.0651	53	2	219,606	109,803	110,813	110,432	1,696	1,712		
Av.									1,702	1.0353	0.21
1F1	0.0634	59	2	26,948	13,474	13,489	13,108	206.7	210.0		
1F2	0.0634	62	2	26,552	13,276	13,281	12,900	203.5	205.8		
1F3	0.0636	65	2	26,671	13,335	13,350	12,969	203.9	207.4		
1F4	0.0636	56	2	27,247	13,623	13,639	13,258	208.3	210.4		
Av.									208.4	215.7	0.61
2F1	0.0632	70	2	246,826	123,413	124,693	124,312	1,967	1,992		
2F2	0.0631	73	2	239,608	119,804	121,024	120,643	1,911	1,937		
2F3	0.0631	76	2	241,925	120,962	122,192	121,811	1,930	1,957		
2F4	0.0631	79	2	245,073	122,536	123,806	123,725	1,960	1,989		
Av.									9,969	2,038	0.20
3FCd1	0.0614	85	2	103,996	51,998	52,224	51,843	844.3	857.2		
3FCd2	0.0614	88	2	71,101	35,550	35,652	35,271	574.4	583.4		
3FCd3	0.0614	91	2	71,125	35,562	35,665	35,284	574.7	584.1		
3FCd4	0.0614	94	2	106,975	53,487	53,722	53,341	868.7	883.3		
Av.									727.0	752.6	0.33
4FCd1	0.0616	97	2	622,737	311,368	319,568	319,187	5,182	5,272		
4FCd2	0.0616	100	2	429,558	214,779	218,699	218,318	3,544	3,608		
4FCd3	0.0616	103	2	423,026	211,513	215,273	214,892	3,489	3,554		
4FCd4	0.0616	108	2	598,986	299,493	307,093	306,712	4,979	5,077		
									4,378	4,532	0.14

Table 6. (Continued)

Reactor run: G April 13, 1962
Power level: 20 watts for 20 minutes
Cadmium covers: 20 mil thickness
Background activity: 381 c/m
Uranium standard: 83,662 counts/2 minutes

Foil	Wgt (gm)	t_w (min)	t_c (min)	Counts	Rate, r (c/m)	r_d (c/m)	r_{-b} (c/m)	r_n (c/m)	$A_{(x)}$ (c/m)	A_{std}	$\% \sigma_s$
1SG	0.0646	59	5	22,154	4,430.8	4,432	4,051	62.71	63.37		
2SG	0.0646	65	5	22,537	4,507.4	4,509	4,128	63.90	64.65		
Av.									64.01	27.527	0.75
3G1	0.0641	73	3	82,967	27,656	27,718	27,337	426.5	432.1	11,894	0.35
4G1	0.0641	77	2	158,506	79,253	79,776	79,395	1,239	1,256	34,574	0.25

Reactor run: H April 13, 1962
Power level: 20 watts for 20 minutes
Cadmium covers: 20 mil thickness
Background activity: 401 c/m
Uranium standard: 83,662 counts/2 minutes

Foil	Wgt (gm)	t_w (min)	t_c (min)	Counts	Rate, r (c/m)	r_d (c/m)	r_{-b} (c/m)	r_n (c/m)	$A_{(x)}$ (c/m)	A_{std}	$\% \sigma_s$
1SH	0.0651	37	5	22,566	4,513	4,514	4,113	63.17	63.59		
2SH	0.0650	43	5	22,804	4,561	4,562	4,161	64.01	64.50		
Av.									64.04	27.514	0.75
3H1	0.0621	(This foil was accidently omitted--correction made)									
3H2	0.0623	151	2	42,827	21,414	21,453	21,052	337.9	347.1		
3H3	0.0623	154	2	41,068	20,534	20,569	20,168	323.7	332.7		
3H4	0.0623	157	2	40,235	20,117	20,151	19,750	317.0	326.0		
3H5	0.0623	160	2	39,979	19,989	20,022	19,621	314.9	324.0		
3H6	0.0623	163	2	40,372	20,186	20,220	19,819	318.1	327.5		

Table 6. (Continued)

Foil	Wgt (gm)	t_w (min)	t_c (min)	Counts	Rate, r (c/m)	r_d (c/m)	r_{-b} (c/m)	r_n (c/m)	A(x) (c/m)	A_{std}	% σ_s
3H7	0.0623	166	2	39,439	19,719	19,752	19,351	310.6	319.9		
3H8	0.0623	169	2	39,075	19,537	19,569	19,168	306.1	315.5		
3H9	0.0623	172	2	39,456	19,728	19,761	19,360	315.1	324.9		
3H10	0.0622	175	2	40,213	20,106	20,140	19,739	317.3	327.3		
3H11	0.0622	178	2	40,407	20,203	20,237	19,836	318.9	329.2		
3H12	0.0622	181	2	43,485	21,742	21,781	21,380	343.7	355.0		
Av.									329.9	9,077	0.50
4H1	0.0629	192	2	122,789	61,394	61,707	61,306	974.7	1006.		
4H2	0.0629	195	2	11,897	55,948	56,208	55,807	887.2	918.5		
4H3	0.0628	198	2	105,416	52,708	52,941	52,540	836.6	866.6		
4H4	0.0628	201	2	104,599	52,299	52,526	52,125	830.0	860.1		
4H5	0.0628	204	2	105,682	52,841	53,074	52,673	838.7	869.6		
4H6	0.0628	223	2	100,766	50,383	50,597	50,196	799.3	831.7		
4H7	0.0628	226	2	106,424	53,212	53,449	53,048	844.7	879.4		
4H8	0.0626	229	2	104,654	52,327	52,555	52,154	833.1	867.7		
4H9	0.0626	231	2	106,177	53,089	53,325	52,924	845.4	880.9		
4H10	0.0626	234	2	106,618	53,309	53,546	53,145	849.0	885.1		
4H11	0.0625	237	2	110,501	55,250	55,505	55,104	881.7	919.8		
4H12	0.0625	240	2	120,672	60,336	60,639	60,238	963.8	1006.		
Av.									899.4	24,750	0.30

Table 6. (Continued)

Foil	Wgt (gm)	t_w (min)	t_c (min)	Counts	Rate, r (c/m)	r_d (c/m)	r_{-b} (c/m)	r_n (c/m)	$A_{(x)}$ (c/m)	A_{std}	% σ_s
Reactor run: I April 17, 1962 Power level: 20 watts for 20 minutes Background activity: 387 c/m Uranium standard: 83,976 counts/20 minutes											
1SI	0.0619	77	5	22,352	4,470.4	4,472	4,085	65.99	66.89		
2SI	0.0619	83	5	23,562	4,712.4	4,714	4,327	69.90	70.94		
Av.									68.91	25.59	0.75
3I1	0.0613	89	2	53,014	26,507	26,565	26,178	427.0	433.8		
3I2	0.0614	92	2	52,423	26,211	26,267	25,880	421.5	428.5		
Av.									431.1	11,020	0.45
4I1	0.0610	95	2	145,324	72,662	73,102	72,715	1,192	1,212		
4I2	0.0610	98	2	144,147	72,073	72,503	72,116	1,182	1,203		
Av.									1,208	30,900	0.26
Reactor run: K April 17, 1962 Power level: 500 watts for 20 minutes Background activity: 357 c/m Uranium standard: 83,357 counts/2 minutes											
1SK	0.605	38	2	195,906	97,953	98,700	98,347	1,626	1,636		
2SK	0.605	41	2	196,307	98,153	98,958	98,601	1,630	1,642		
Av.									1,639	1.07504	0.24
1K1	0.0637	274	2	21,888	10,944	10,954	10,597	166.4	174.7		
1K2	0.0637	277	2	20,577	10,289	10,298	9,941	156.1	164.0		
1K3	0.0637	280	2	20,801	10,400	10,410	10,053	157.8	165.9		
1K4	0.0637	283	2	20,129	10,064	10,073	9,716	152.5	160.4		
1K5	0.0637	286	2	20,129	10,064	10,073	9,716	152.5	160.5		

Table 6. (Continued)

Foil	Wgt (gm)	t_w (min)	t_c (min)	Counts	Rate, r (c/m)	r_d (c/m)	r_{-b} (c/m)	r_n (c/m)	$A_{(x)}$ (c/m)	A_{std}	% σ_s
1K6	0.0638	289	2	20,089	10,045	10,054	9,997	156.7	165.0		
1K7	0.0638	292	2	20,869	10,434	10,444	10,087	158.1	166.6		
1K8	0.0638	311	2	20,693	10,347	10,355	9,998	156.7	165.2		
1K9	0.0639	298	2	20,168	10,084	10,093	9,736	152.4	160.7		
1K10	0.0639	301	2	20,123	10,061	10,070	9,713	152.0	160.4		
1K11	0.0640	304	2	20,618	10,309	10,318	9,961	155.6	164.3		
1K12	0.0641	307	2	21,212	10,606	10,616	10,259	160.0	169.0		
Av.									164.7	177.1	0.70
2K1	0.0621	331	2	193,499	96,749	97,529	97,172	1,565	1,660		
2K2	0.0621	334	2	190,765	95,382	96,142	95,785	1,542	1,637		
2K3	0.0622	337	2	183,661	91,830	92,530	92,173	1,482	1,574		
2K4	0.0623	340	2	182,569	91,284	91,977	91,620	1,471	1,563		
2K5	0.0623	343	2	182,560	91,280	91,973	91,616	1,471	1,564		
2K6	0.0623	346	2	181,659	90,829	91,514	91,157	1,463	1,556		
2K7	0.0624	349	2	181,222	90,611	91,295	90,938	1,457	1,550		
2K8	0.0624	352	2	184,709	92,354	93,064	92,707	1,486	1,582		
2K9	0.0625	355	2	185,544	92,772	93,489	93,132	1,490	1,587		
2K10	0.0626	358	2	185,924	92,962	93,681	93,324	1,491	1,589		
2K11	0.0627	361	2	192,706	96,353	97,125	96,768	1,543	1,646		
2K12	0.0627	364	2	197,759	98,879	99,989	99,632	1,589	1,696		
Av.									1,600	1,720	0.23

Table 6. (Continued)

Foil	Wgt (gm)	t_w (min)	t_c (min)	Counts	Rate, r (c/m)	r_d (c/m)	r_{-b} (c/m)	r_n (c/m)	$A_{(x)}$ (c/m)	A_{std}	% σ_s
3CdK1	0.0630	380	2	91,798	45,899	46,074	45,717	725.7	776.6		
3CdK2	0.0630	383	2	55,643	27,821	27,884	27,527	436.9	467.8		
3CdK3	0.0630	386	2	48,723	24,361	24,410	24,053	381.8	409.0		
3CdK4	0.0631	389	2	45,194	22,597	22,639	22,282	353.1	378.5		
3CdK5	0.0631	392	2	44,231	22,115	22,155	22,798	361.3	387.5		
3CdK6	0.0632	395	2	43,147	21,573	21,612	21,255	336.3	360.8		
3CdK7	0.0632	398	2	42,191	21,096	21,133	20,776	328.7	352.9		
3CdK8	0.0633	401	2	44,577	22,288	22,329	21,972	347.1	372.8		
3CdK9	0.0634	404	2	46,129	23,064	23,108	22,751	358.8	385.6		
3CdK10	0.0634	407	2	48,807	24,409	24,458	24,101	380.1	408.8		
3CdK11	0.0635	410	2	54,819	27,409	27,470	27,113	427.0	459.4		
3CdK12	0.0635	413	2	92,697	46,349	46,529	46,172	727.1	782.7		
Av.									461.9	496.6	0.41
4CdK1	0.0615	520	2	507,378	253,689	259,000	258,643	4,206	4,614		
4CdK2	0.0616	523	2	312,912	156,456	158,500	158,149	2,567	2,818		
4CdK3	0.0616	526	2	274,743	137,372	138,842	138,485	2,248	2,469		
4CdK4	0.0617	529	2	261,034	130,517	131,957	131,600	2,133	2,344		
4CdK5	0.0617	531	2	246,741	123,371	124,656	124,299	2,015	2,215		
4CdK6	0.0617	534	2	243,587	121,793	123,020	122,666	1,988	2,187		
4CdK7	0.0617	537	2	242,933	121,467	122,697	122,340	1,983	2,192		
4CdK8	0.0617	540	2	242,934	121,467	122,697	122,340	1,983	2,203		
4CdK9	0.0618	543	2	257,501	128,750	130,160	129,803	2,100	2,347		
4CdK10	0.0619	546	2	257,627	128,813	130,223	129,866	2,098	2,358		
4CdK11	0.0620	549	2	313,327	156,664	158,714	158,357	2,554	2,883		
4CdK12	0.0620	552	2	515,341	257,670	263,323	262,966	4,241	4,814		
Av.									2,787	2,996	0.19

Table 6. (Continued)

Foil	Wgt (gm)	t_w (min)	t_c (min)	Counts	Rate, r (c/m)	r_d (c/m)	r_{-b} (c/m)	r_n (c/m)	$A_{(x)}$ (c/m)	A_{std}	$\%\sigma_s$
				Reactor run: L April 19, 1962 Power level: 20 watts for 20 minutes Background activity: 387 c/m Uranium standard: 83,890 counts/2 minutes							
1SL	0.0655	300	5	22,520	4,504	4,505	4,118	62.87	66.33		
2SL	0.0655	306	5	22,613	4,525	4,526	4,139	63.19	66.73		
Av.									66.53	26.4842	0.75
3L1	0.0636	334	2	49,866	24,933	24,984	24,597	386.7	410.4		
3L2	0.0636	337	2	47,228	23,614	23,660	23,273	365.9	388.6		
3L3	0.0637	340	2	46,888	23,444	23,489	23,102	362.7	385.4		
3L4	0.0637	346	2	46,907	23,453	23,498	23,111	362.8	385.9		
Av.									392.6	10,398	0.46
4L1	0.0640	315	2	136,394	68,197	68,583	68,196	1,066	1,128		
4L2	0.0640	318	2	128,425	64,212	64,555	64,168	1,003	1,062		
4L3	0.0641	321	2	128,671	64,335	64,678	64,291	1,003	1,062		
4L4	0.0641	324	2	128,659	64,329	64,672	64,285	1,004	1,064		
Av.									1,079	28,576	0.28

Table 6. (Continued)

Foil	Wgt (gm)	t_w (min)	t_c (min)	Counts	Rate, r (c/m)	r_d (c/m)	r_{-b} (c/m)	r_n (c/m)	$A_{(x)}$ (c/m)	A_{std}	$\% \sigma_s$

Reactor run: M April 20, 1962
Power level: 600 watts for 20 minutes
Cadmium covers: 20 mil thickness
Background activity: 355 c/m
Uranium standard: 83,885 counts/2 minutes

Foil	Wgt (gm)	t_w (min)	t_c (min)	Counts	Rate, r (c/m)	r_d (c/m)	r_{-b} (c/m)	r_n (c/m)	$A_{(x)}$ (c/m)	A_{std}	$\% \sigma_s$
1SM	0.0647	28	2	218,064	109,032	110,037	109,652	1,695	1,703		
2SM	0.0648	31	2	213,570	106,785	107,730	107,375	1,657	1,666		
Av.									1,684	1.0460	0.22
3SM	0.0651	17	10	20,154	2,015	2,015	1,660	25.50	25.58		
4SM	0.0652	60	10	20,739	2,074	2,074	1,719	26.36	26.64		
Av.									26.11	27.300	1.56
1M1	0.0617	270	2	23,444	11,722	11,734	11,379	184.4	193.5		
1M2	0.0618	273	2	22,970	11,485	11,497	11,142	180.3	189.3		
1M3	0.0619	277	2	22,701	11,351	11,362	11,007	177.8	186.8		
1M4	0.0620	280	2	22,568	11,284	11,295	10,940	176.5	185.6		
1M5	0.0620	283	2	22,439	11,219	11,229	10,874	175.4	184.5		
1M6	0.0621	286	2	22,453	11,227	11,237	10,872	175.1	184.3		
1M7	0.0622	289	2	22,744	11,372	11,383	11,028	177.3	186.7		
1M8	0.0622	292	2	22,635	11,317	11,328	10,973	176.4	185.8		
Av.									187.0	195.6	0.67

Table 6. (Continued)

Foil	Wgt (gm)	t_w (min)	t_c (min)	Counts	Rate, r (c/m)	r_d (c/m)	r_{-b} (c/m)	r_n (c/m)	$A_{(x)}$ (c/m)	A_{std}	$\% \sigma_s$
2M1	0.0607	334	2	210,451	105,225	106,157	105,802	17,430	18,500		
2M2	0.0607	331	2	206,833	103,417	104,317	103,952	17,126	18,170		
2M3	0.0607	328	2	203,397	101,698	102,548	102,193	16,836	17,850		
2M4	0.0608	310	2	205,515	102,757	103,697	103,342	17,000	17,970		
2M5	0.0608	313	2	201,996	100,998	102,048	101,693	16,726	17,690		
2M6	0.0609	316	2	205,564	102,782	103,672	103,317	16,965	17,950		
2M7	0.0609	319	2	206,073	103,036	103,926	103,571	17,007	18,000		
2M8	0.0609	322	2	211,405	105,702	106,642	106,287	17,453	18,480		
Av.									18,076	1,891	0.22
3CdM1	0.0613	358	2	94,121	47,062	47,248	46,893	765.0	815.5		
3CdM2	0.0613	361	2	58,684	29,342	29,411	29,056	474.0	505.5		
3CdM3	0.0614	364	2	53,536	26,768	26,831	26,476	431.2	460.1		
3CdM4	0.0614	367	2	51,208	25,604	25,658	25,303	412.1	440.0		
3CdM5	0.0614	370	2	52,069	26,035	26,082	25,727	419.0	447.6		
3CdM6	0.0614	373	2	54,002	27,001	27,061	26,706	435.0	464.9		
3CdM7	0.0015	377	2	59,331	29,666	29,738	29,383	477.8	511.0		
3CdM8	0.0615	380	2	94,069	47,035	47,120	46,765	760.4	813.7		
Av.									557.3	582.9	0.41
4CdM1	0.0594	394	2	532,392	266,196	272,206	271,851	4,577	4,910		
4CdM2	0.0594	397	2	334,575	167,287	170,287	169,932	2,861	3,071		
4CdM3	0.0595	400	2	305,248	152,624	155,344	154,989	2,605	2,798		
4CdM4	0.0598	403	2	294,319	147,159	148,979	148,624	2,485	2,670		
4CdM5	0.0600	406	2	299,112	149,556	151,436	151,081	2,518	2,707		
4CdM6	0.0601	410	2	304,665	152,333	155,063	154,708	2,574	2,769		
4CdM7	0.0605	413	2	341,312	170,656	173,281	172,826	2,857	3,075		
4CdM8	0.0607	416	2	542,343	271,172	276,412	276,057	4,548	4,898		
Av.									3,362	3,517	0.18

Table 6. (Continued)

Foil	Wgt (gm)	t_w (min)	t_c (min)	Counts	Rate, r (c/m)	r_d (c/m)	r_{-b} (c/m)	r_n (c/m)	A(x) (c/m)	A_{std}	% σ_s
				Reactor run: N April 19, 1962 Power level: 20 watts for 20 minutes Background activity: 341 c/m Uranium standard: 83,278 counts/2 minutes							
1SN	0.0649	366	5	21,800	4,360	4,361	4,020	61.94	66.12		
2SN	0.0649	372	5	22,696	4,539	4,540	4,199	64.67	69.11		
Av.									67.61	26.0593	0.74
3N1	0.0642	378	2	46,818	23,409	23,454	23,113	360.0	385.1		
3N2	0.0643	381	2	44,913	22,456	22,498	22,157	344.6	368.9		
3N3	0.0643	384	2	43,802	21,901	21,941	21,600	335.9	359.7		
3N4	0.0643	387	2	43,007	21,503	21,541	21,200	329.7	353.3		
3N5	0.0644	390	2	43,723	21,862	22,902	21,561	334.8	388.9		
3N6	0.0645	393	2	43,642	21,821	21,861	21,520	333.6	357.8		
3N7	0.0646	396	2	43,749	21,874	21,914	21,573	333.9	358.3		
3N8	0.0646	399	2	46,310	23,155	23,199	22,758	352.3	378.3		
Av.									365.0	9,512	0.48
4N1	0.0610	410	2	122,489	61,244	61,556	61,215	1004.	1080.		
4N2	0.0611	413	2	113,552	56,776	57,044	56,703	928.0	998.9		
4N3	0.0611	416	2	110,279	55,139	55,394	55,053	901.0	970.4		
4N4	0.0611	419	2	109,665	54,832	55,082	54,741	895.9	965.4		
4N5	0.0611	422	2	108,804	54,402	54,649	54,308	888.8	958.3		
4N6	0.0612	425	2	111,438	55,719	55,977	55,636	909.1	980.7		
4N7	0.0612	428	2	112,130	56,065	56,327	55,986	914.8	987.4		
4N8	0.0613	431	2	122,067	61,033	61,343	61,002	995.1	1075.		
Av.									1002.	26,111	0.30

Table 6. (Continued)

Foil	Wgt (gm)	t_w (min)	t_c (min)	Counts	Rate, r (c/m)	r_d (c/m)	r_{-b} (c/m)	r_n (c/m)	$A_{(x)}$ (c/m)	A_{std}	$\% \sigma_s$
				<u>Reactor run: O April 20, 1962</u> Power level: 10 kw for 20 minutes Background activity: 332 c/m Uranium standard: 83,885 counts/2 minutes							
3SO	0.0659	201	2	67,046	33,523	33,614	33,282	505.0	523.5		
4SO	0.0657	204	2	67,890	33,945	34,038	33,706	513.0	532.0		
Av.									527.8	0.05175	0.39
1Cd01	0.0656	81	60	29,674	494.6	494.6	162.6	2.479	2.515	0.1301	17.8
2Cd01	0.0655	77	2	39,804	19,902	19,935	19,602	299.3	303.4	15.70	0.51
				<u>Reactor run: P April 24, 1962</u> Power level: 500 watts for 20 minutes Cadmium covers: 10 mil thickness Background activity: 322 c/m Uranium standard: 83,481 counts/2 minutes							
1SP	0.0630	31	2	208,296	104,148	105,058	104,736	1,662	1,671		
2SP	0.0630	34	2	210,648	105,324	106,254	105,932	1,681	1,691		
Av.									1,681	1.04818	0.21
3PCd1	0.0649	38	2	178,441	89,220	89,880	89,558	1,380	1,389	1.456	0.23

Table 6. (Continued)

<u>Reactor run: Q April 26, 1962</u>
Power level: 500 watts for 20 minutes
Cadmium covers: 40 mil thickness
Background activity: 317 c/m
Uranium standard: 83,485 counts/2 minutes

Foil	Wgt (gm)	t_w (min)	t_c (min)	Counts	Rate, r (c/m)	r_d (c/m)	r_{-b} (c/m)	r_n (c/m)	$A_{(x)}$ (c/m)	A_{std}	$\%\sigma_s$
1SQ	0.0625	90	2	214,657	107,328	108,296	107,979	1,728	1,756		
2SQ	0.0625	93	2	213,164	106,582	107,522	107,205	1,715	1,744		
Av.									1,760	1.00113	0.21
3QCdL	0.0638	96	2	150,770	75,385	75,858	75,541	1,184	1,204	1.205	0.26

<u>Reactor run: R April 26, 1962</u>
Power level: 500 watts for 20 minutes
Cadmium covers: 60 mil thickness
Background activity: 335 c/m
Uranium standard: 83,485 counts/2 minutes

Foil	Wgt (gm)	t_w (min)	t_c (min)	Counts	Rate, r (c/m)	r_d (c/m)	r_{-b} (c/m)	r_n (c/m)	$A_{(x)}$ (c/m)	A_{std}	$\%\sigma_s$
1SR	0.0626	40	2	210,847	105,424	106,359	105,024	1,694	1,706		
2SR	0.0626	43	2	211,962	105,981	106,823	106,488	1,701	1,714		
Av.									1,710	1.03040	0.21
3RCdl	0.0638	46	2	149,152	74,576	75,051	74,716	1,171	1,181	1.217	0.26

Table 6. (Continued)

Foil	Wgt (gm)	t_w (min)	t_c (min)	Counts	Rate, r (c/m)	r_d (c/m)	r_{-b} (c/m)	r_n (c/m)	$A_{(x)}$ (c/m)	A_{std}	$\%\sigma_s$
				Reactor run: S May 9, 1962 Power level: 500 watts for 20 minutes Cadmium covers: 30 mil thickness Background activity: 336 c/m Uranium standard: 83,694 counts/2 minutes							
1SS	0.0629	37	2	212,658	106,329	107,274	106,938	1,700	1,711		
2SS	0.0629	40	2	215,823	107,911	108,906	108,570	1,726	1,738		
Av.									1,725	1.02144	0.21
3CdS1	0.0637	46	2	159,584	79,792	80,322	79,986	1,256	1,266	1293	0.25
				Reactor run: T May 9, 1962 Power level: 500 watts for 20 minutes Cadmium covers: 50 mil thickness Background activity: 292 c/m Uranium standard: 83,957 counts/2 minutes							
1ST	0.0629	485	2	206,099	103,049	103,944	103,552	1,646	1,794		
2ST	0.0629	488	2	202,684	101,342	102,192	101,900	1,620	1,767		
Av.									1,781	0.98933	0.22
3CdT1	0.0632	500	2	139,254	69,627	70,032	69,740	1,103	1,206	1193	0.27

Table 6. (Continued)

Foil	Wgt (gm)	t_w (min)	t_c (min)	Counts	Rate, r (c/m)	r_d (c/m)	r_{-b} (c/m)	r_n (c/m)	$A_{(x)}$ (c/m)	A_{std}	% σ_s
<u>Reactor run: U May 23, 1962</u> Power level: 500 watts for 20 minutes Cadmium covers: 60 mil thickness Background activity: 316 c/m Uranium standard: 83,968 counts/2 minutes											
1SU	0.0622	107	2	203,977	101,989	102,859	102,543	1,649	1,681		
2SU	0.0624	110	2	206,026	103,013	103,903	103,587	1,660	1,693		
Av.									1,687	1.04075	0.22
3CdU1	0.0632	116	2	144,458	72,229	72,664	72,348	1,145	1,169	1,217	0.27
<u>Reactor run: V May 24, 1962</u> Power level: 500 watts for 20 minutes Cadmium covers: 80 mil thickness Background activity: 317 c/m Uranium standard: 83,853 counts/2 minutes											
1SV	0.0662	59	2	229,232	114,616	115,716	115,399	1,743	1,761		
2SV	0.0667	66	2	229,288	114,644	115,744	115,427	1,731	1,751		
									1,756	1.00342	0.18
3CdV1	0.0654	51	2	145,542	72,771	73,211	72,894	1,115	1,125	1,129	0.26